REVIEW ARTICLE

The ESCRT machinery: From the plasma membrane to endosomes and back again

Amber L. Schuh and Anjon Audhya

Department of Biomolecular Chemistry, University of Wisconsin-Madison School of Medicine and Public Health, Madison, WI, USA

Abstract

The manipulation and reorganization of lipid bilayers are required for diverse cellular processes, ranging from organelle biogenesis to cytokinetic abscission, and often involves transient membrane disruption. A set of membrane-associated proteins collectively known as the endosomal sorting complex required for transport (ESCRT) machinery has been implicated in membrane scission steps, which transform a single, continuous bilayer into two distinct bilayers, while simultaneously segregating cargo throughout the process. Components of the ESCRT pathway, which include 5 distinct protein complexes and an array of accessory factors, each serve discrete functions. This review focuses on the molecular mechanisms by which the ESCRT proteins facilitate cargo sequestration and membrane remodeling and highlights their unique roles in cellular homeostasis.

Introductory remarks

The collection of endosomal sorting complex required for transport (ESCRT) proteins consists of more than 30 gene products, many of which interact directly to generate distinct molecular machines that carry out a variety of cellular activities (Table 1). While the early-acting ESCRT complexes (ESCRT-0, ESCRT-I and ESCRT-II) assemble stably within the cytoplasm, the late-acting modules (ESCRT-III and Vps4-Vta1, which we refer to as ESCRT-IV) function specifically on membranes. A large proportion of these components have been characterized at angstrom resolution (reviewed extensively in (Hurley, 2010; Hurley & Emr, 2006; McCullough et al., 2013; Williams & Urbé, 2007), enabling a detailed understanding about how they associate with one another. Combined with genetic- and reconstitution-based studies, the assembly hierarchy of the ESCRT machinery on endosomal membranes has been determined, with ESCRT-0 acting most upstream to recruit ESCRT-I. The ESCRT-I complex engages ESCRT-II, which then nucleates ESCRT-III polymerization via the activation of the ESCRT-III subunit Vps20. ESCRT-IV ultimately disassembles the ESCRT-III complex to recycle its subunits. It is now clear that the ESCRT-III complex facilitates changes in membrane architecture, while the upstream components target ESCRT-III assembly to specific sites within cells. However, the field has yet to reach a consensus on the mechanisms by which the ESCRT machinery acts.

ESCRT-mediated membrane scission is an evolutionarily conserved process that is observed in disparate species, from archaea to eukaryotes. In all cases, ESCRT polymers assemble on the cytoplasmic surface of organelles to mediate membrane remodeling and ultimately facilitate topologically similar rearrangements. A series of genetic screens in yeast uncovered the majority of ESCRT subunits, all of which participate in the delivery of soluble and integral membrane hydrolytic enzymes to the lysosome lumen (Raymond et al., 1992; Rieder et al., 1996). Individual inhibition of these factors results in a distinctive phenotype that is highlighted by the formation of aberrant endosomes, consisting of numerous stacks of flattened cisternae, commonly known as class E compartments. While this effect is largely uniform in yeast, depletion studies in human cells reveal more variability, including the appearance of enlarged, swollen endosomes in some cases (Komada & Soriano, 1999; Raiborg et al., 2008). Irrespective of the morphological differences, the underlying mechanism governing the superfluous addition of membrane to endosomes may be shared. Sustained activity of the Rab5 GTPase promotes endosome fusion, resulting in organelles that have a similar surface area to those seen following ESCRT depletion in human cells (Stenmark et al., 1994; Wegner et al., 2010). Moreover, function of the Rab5 isoform Vps21 is necessary to generate class E compartments in yeast cells that lack ESCRT components (Russell et al., 2012). These studies suggest that ESCRT dysfunction leads to an increase in Rab5 activity on endosomes, driving membrane accumulation and altering endosome morphology.

Address for correspondence: Anjon Audhya, Department of Biomolecular Chemistry, University of Wisconsin-Madison School of Medicine and Public Health, 440 Henry Mall, 5214 Biochemical Sciences, Madison, WI 53706, USA. Tel: (608) 262-3761. Fax: (608) 262-5253. E-mail: audhya@wisc.edu

Table 1. Key components of the ESCRT machinery and their interacting partners.

Metazoan protein	Yeast protein	Interacting partners	Motifs/domains
ESCRT-0			
Hrs	Vps27	PI3P, Ubiquitin, Tsg101, STAM, Clathrin	VHS, FYVE, DUIM, PxxP, CC, CB
STAM 1,2	Hse1	Ubiquitin, DUBs, Hrs	VHS, UIM, SH3, CC
ESCRT-I			
Tsg101	Vps23	Hrs, Alix, Ubiquitin, Cep55, Mvb12, Vps28, Vps27	UEV, PRR, CC
Mvb12 A,B; UBAP1	Mvb12	PS, Tsg101, Vps37, Ubiquitin (yeast/UBAP1)	MABP, UMA
Vps37 A,B,C,D	Vps37	Tsg101, Mvb12, Acidic Phospholipids	NTD, PRR
Vps28	Vps28	Tsg101, Vps36	CTD
ESCRT-II			
Vps36 (EAP45)	Vps36	PI3P, Ubiquitin, Vps28, Vps22, Vps25	GLUE, WH, NZF (yeast)
Vps22 (EAP30)	Vps22	Acidic Phospholipids, Vps25, Vps36	HD, WH
Vps25 (EAP20)	Vps25	Vps22, Vps36, Vps20	WH
ESCRT-III (Core Components)			
hVps20 (CHMP6)	Vps20	Vps25, Vps32, Vps4	MIM2
hVps32 (CHMP4 A,B,C)	Vps32 (Snf7)	Vps20, Vps24, Vps4, Alix, CHMP7, DUBs	MIM2
hVps24 (CHMP3)	Vps24	Vps32, Vps2, Vps4, Did2, PI3,5P$_2$, DUBs	MIM1
hVps2 (CHMP2 A,B)	Vps2	Vps24, Vps4, Did2	MIM1
ESCRT-III (Additional Factors)			
hDid2 (CHMP1 A,B)	Did2 (Vps46)	Ist1, Vps4, Vta1, Vps24, Vps2, DUBs, Spastin	MIM1
Ist1	Ist1	Vps4, Did2, Vta1	MIM1, MIM2
hVps60 (CHMP5)	Vps60 (Mos10)	Vta1, Vps4	Unclassified MIM
CHMP7	–	CHMP4B	MIM1, MIM2
ESCRT-IV			
Vps4 A,B (SKD1)	Vps4	Vps20, Vps32, Vps24, Vps2, Did2, Vta1, Ist1, Vps60	MIT, AAA, β-Domain
LIP5	Vta1	Vps4, Vps60, Did2, Ist1, Vps20, Vps32, Vps24, Vps2	MIT, VSL
Accessory			
Alix (AIP1)	Bro1 (Vps31)	Tsg101, Vps32, Cep55, DUBs	Bro1, PRR

Components of the ESCRT complexes and accessory factors are shown, with both metazoan and yeast nomenclatures provided. Also the important domains found in each factor and characterized binding partners for ESCRT components are listed. Please refer to the text for references. Abbreviations: Clathrin Binding (CB), Coiled-Coil (CC), C-Terminal Domain (CTD), Deubiquitinating Enzyme (DUB), Double-Sided Ubiquitin-Interacting Motif (DUIM), Fab-1, YGL023, Vps27, and EEA1 (FYVE), GRAM-Like Ubiquitin-binding in EAP45 (GLUE), Helical-Domain (HD), Mvb12-associated β-prism (MABP), Microtubule Interacting and Transport (MIT), N-Terminal Domain (NTD), Npl4 zinc finger (NZF), Phosphatidylinositol-3-Phosphate (PI3P), Proline Rich Region (PRR), Src homology-3 (SH3), Ubiquitin E2 variant (UEV), Ubiquitin Interacting Motif (UIM), Ubap1-Mvb12-Associated (UMA), Vps27p, Hrs, and STAM (VHS), Winged-Helix (WH).

Although a function for the ESCRT machinery was initially discovered in the endosomal system, its most ancient activity likely originates at the site of cell division (Samson *et al.*, 2008). Homologues of several ESCRT-III and ESCRT-IV subunits have been identified throughout the crenarchaeal phylum, and those in *Sulfolobus acidocaldarius* were shown to direct the process of cytokinesis (Ellen *et al.*, 2009; Lindås *et al.*, 2008; Makarova *et al.*, 2010). In an analogous manner, the ESCRT machinery plays important roles during cytokinetic abscission in animal cells and potentially plants (Carlton & Martin-Serrano, 2007; Morita *et al.*, 2007b; Spitzer *et al.*, 2006). In contrast, the yeast ESCRT complexes have not been found to participate directly in cytokinesis, but may instead contribute to the process of cell division through their roles in endocytic trafficking (McMurray *et al.*, 2011). The absence of a specific role for the ESCRT machinery in yeast cytokinesis may be due to the lack of an appropriate adaptor protein. Mammalian cells use the microtubule bundling protein Cep55 to direct ESCRT components to the midbody, while archaea take advantage of an unrelated factor, CdvA (Carlton & Martin-Serrano, 2007; Dobro *et al.*, 2013; Morita *et al.*, 2007b; Samson *et al.*, 2011). These findings suggest that the evolution of adaptors required for recruitment of ESCRT components to the cell division plane occurred independently in archaea and eukaryotes. Surprisingly, Cep55 homologues

have not been identified outside of vertebrates, indicating that alternative mechanisms to enable ESCRT components to function in cytokinesis must exist in other metazoan organisms (Green *et al.*, 2013). Additionally, non-host adaptors can also recruit the ESCRT machinery to the cell surface to support the budding of numerous enveloped viruses (reviewed extensively in McCullough *et al.*, 2013; Meng & Lever, 2013; Votteler & Sundquist, 2013; Weissenhorn *et al.,* 2013). Based on these data, it is reasonable to assume that other, yet to be identified adaptors exist, which can recruit ESCRT components to additional subcellular locations.

The goal of this review is to highlight recent developments that have shed light on our understanding of the mechanisms by which the ESCRT machinery acts. While we refer readers to other excellent reviews that have recently described the role of the ESCRT machinery in the budding of enveloped viruses (McCullough *et al.*, 2013; Meng & Lever, 2013; Votteler & Sundquist, 2013; Weissenhorn *et al.*, 2013), we will focus on the normal, physiological roles of ESCRT complexes in regulating the transport of membrane-associated proteins through the endocytic system and membrane abscission following cytokinesis. In particular, we will explore mechanisms that regulate the function and distribution of ESCRT components. It is now clear that the ESCRT machinery is not restricted to endosomes, as is suggested by its name.

RIGHTSLINK()

Rather, a combination of protein and lipid interactions can direct ESCRT activity to multiple intracellular sites to facilitate membrane remodeling and budding reactions that sequester cargoes from the cytoplasm.

ESCRT-mediated cargo sorting in the endolysosomal system

Historically, the ESCRT system was first described as a network of complexes that function cooperatively to sort integral membrane proteins modified by ubiquitin (reviewed extensively in Hurley & Emr, 2006; Raiborg & Stenmark, 2009; Saksena et al., 2007; Shields & Piper, 2011). The attachment of ubiquitin functions as a sorting signal to direct cargoes into intralumenal vesicles (ILVs) within endosomes, which ultimately fuse with lysosomes (Katzmann et al., 2001; Kölling & Hollenberg, 1994; Reggiori & Pelham, 2001). Incoming cargoes from the cell surface and the Golgi apparatus are among the best characterized substrates of this degradative pathway. In both cases, E3 ubiquitin ligases transfer ubiquitin onto one or more cytosol-facing lysine residues within substrates (reviewed extensively in Bonifacino & Traub, 2003; Hicke & Dunn, 2003; Hurley & Stenmark, 2011; Piper & Lehner, 2011). Although a single ubiquitin is sufficient for sorting into ILVs (Haglund et al., 2003; Stringer & Piper, 2011; Urbanowski & Piper, 2001), many cargoes undergo polyubiquitin-modification in vivo (Duncan et al., 2006; Geetha et al., 2005; Huang et al., 2006). In the case of epidermal growth factor receptor (EGFR), ligand stimulation results in a greater than 20-fold increase in ubiquitin modification relative to basal conditions (Huang et al., 2013). The majority of EGFR-associated ubiquitin is in the form of K63-linked chains (Argenzio et al., 2011; Huang et al., 2006, 2013; Meijer & van Leeuwen 2011), although K48-, K11- and K29-linked chains have also been observed (Huang et al., 2006). Dependencies on the presence of each chain type have yet to be determined for EGFR sorting. However, these data raise the possibility that an ubiquitin code acts to facilitate the segregation of EGFR when it transits through the endolysosomal system. Additionally, deubiquitinating enzymes (DUBs) and other ubiquitin ligases can further modify cargoes to specify their fate (Amerik et al., 2000; Ren et al., 2007; Shenoy & Lefkowitz, 2003). Thus, initial ubiquitin-modification does not necessarily target a protein for destruction, as subsequent editing can redirect its transport away from deposition into ILVs. A prime example of this phenomenon was demonstrated for AMSH, a DUB that interacts directly with components of the ESCRT machinery (Agromayor & Martin-Serrano, 2006; Kato et al., 2000; McCullough et al., 2004, 2006; Solomons et al., 2011; Tanaka et al., 1999). Depletion of AMSH, which alters the balance of E3 ligase/DUB activity in the endosomal system, enhances the degradation of EGFR (Bowers et al., 2006; McCullough et al., 2004), presumably by inhibiting the removal of ubiquitin from EGFR and thereby preventing its ability to recycle. However, the roles of DUBs in cargo sorting may not be so straightforward. Depletion of UBPY, another DUB that associates with ESCRT components (Kato et al., 2000; Row et al., 2007), has been shown to both accelerate and slow the rate of EGFR degradation

(Bowers et al., 2006; Mizuno et al., 2005; Row et al., 2006). A basis for these contradictory findings remains unclear. However, one possibility is that DUBs not only target cargoes, but also components of the ESCRT machinery itself, which have been shown to be ubiquitin-modified by specific E3 ligases (e.g. Tal) in vivo (Amit et al., 2004; Jiao et al., 2009; Katz et al., 2002; Kim et al., 2007; Marchese et al., 2003). Attachment of ubiquitin to ESCRT subunits results in their inactivation (Hoeller et al., 2006; McDonald & Martin-Serrano, 2008), and DUB activity may therefore relieve inhibition of ESCRT-mediated sorting independently of ubiquitin removal from cargo. Alternatively, UBPY has also been proposed to disrupt binding of early-acting ESCRT components to HD-PTP, a member of the Bro1 family of accessory ESCRT proteins that regulates EGFR sorting at endosomes. By doing so, UBPY promotes the transfer of EGFR to late acting ESCRT complexes, while simultaneously facilitating the removal of ubiquitin from EGFR prior to its deposition into ILVs (Ali et al., 2013). This enables recycling of ubiquitin for future rounds of sorting. Thus, depending on the cell type, the interplay of DUB and ubiquitin ligase activities likely fine tune cargo sorting pathways, providing the high level of regulation necessary to control integral membrane protein homeostasis.

Members of the Cbl family of E3 ligases govern ubiquitin-modification of activated EGFR (Levkowitz et al., 1998, 1999; Waterman et al., 1999; Yokouchi et al., 1999). Although Cbl can associate directly with the ligand-bound receptor using a phosphotyrosine binding motif (Lill et al., 2000), it also interacts with Grb2, which acts as an EGFR-associated adaptor (Donovan et al., 1996; Meisner & Czech, 1995; Waterman et al., 2002). More generally, given the several thousand substrates that undergo lysosomal-mediated degradation, perhaps it is not surprising that a large family of adaptors for E3 ubiquitin ligases have evolved. For example, members of the Nedd4 family of E3 ligases have been shown to associate with beta-arrestin 2, which acts as a cargo-specific adaptor that enables ubiquitin modification of the beta2-adrenergic receptor following agonist stimulation (Han et al., 2013; Shenoy et al., 2008). Analogously, several arrestin-related trafficking adaptors (ARTs) have been discovered to function in the downregulation of specific cell surface proteins (Lin et al., 2008). Thus, the arrestins and ARTs represent a large group of adaptors that facilitate recognition of substrates by E3 ligases. Additionally, members of both families of adaptors associate directly with components of the ESCRT machinery, coupling E3 ligase activity to ESCRT function (Herrador et al., 2010; Malik & Marchese, 2010; Rauch & Martin-Serrano, 2011).

Early-acting complexes of the ESCRT machinery are ideally suited to recognize and sequester ubiquitin-modified cargoes (Bishop et al., 2002). Each harbors at least one ubiquitin-binding domain. However, based on interaction studies with soluble ubiquitin, the affinities for these domains are relatively weak, ranging from approximately 100-500 μM (Alam et al., 2004; Garrus et al., 2001; Mayers et al., 2011; Ren & Hurley, 2010; Slagsvold et al., 2005). Nevertheless, mutations that specifically inhibit ESCRT-mediated ubiquitin binding substantially impair cargo sorting to lysosomes, arguing a direct role for these domains in vivo
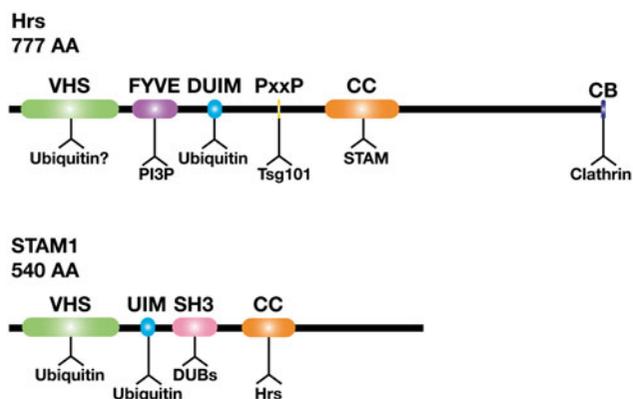
Figure 1. Domain organization of the ESCRT-0 subunits. Illustrations highlight the key domains within Hrs and STAM and their major interaction partners. In mammals, two isoforms of STAM are typically expressed (STAM1 and STAM2). Abbreviations: Clathrin Binding (CB), Coiled-Coil (CC), Double-Sided Ubiquitin-Interacting Motif (DUIM), Fab-1, YGL023, Vps27, and EEA1 (FYVE), Phosphatidylinositol-3-Phosphate (PI3P), Src homology-3 (SH3), Ubiquitin Interacting Motif (UIM), Vps27p, Hrs, and STAM (VHS). (see colour version of this figure at www.informahealthcare.com/bmg).

(Alam *et al.*, 2004; Bilodeau *et al.*, 2003; Ren & Hurley, 2010; Shields *et al.*, 2009; Shih *et al.*, 2002)

Both components of the ESCRT-0 complex, Hrs and STAM, contain ubiquitin-binding domains (Bilodeau *et al.*, 2003; Mizuno *et al.*, 2003) (Figure 1). The Hrs DUIM exhibits the tightest affinity for ubiquitin (~127 μM based on isothermal titration calorimetry experiments using the intact complex) and can engage two ubiquitin molecules simultaneously (Hirano *et al.*, 2006; Mayers *et al.*, 2011). In a similar manner, the UIM and VHS domains of STAM can also associate with ubiquitin, albeit with weaker affinities (Ren & Hurley, 2010). In all cases, the interactions with mono-ubiquitin are not cooperative (Mayers *et al.*, 2011). However, the affinity of intact ESCRT-0 for tetraubiquitin (K63-linked) is approximately seven-fold higher, suggesting that cargoes modified with multiple ubiquitin molecules are likely to bind more avidly to ESCRT-0 through multiple simultaneous interactions (Ren & Hurley, 2010). It is important to note that in most cases, measured affinities underestimate the thermodynamic parameters of ESCRT-0 associations with native cargoes. Since the substrate is integral to the membrane and not freely diffusible, equilibrium constants determined in solution must be converted to measurements in two dimensions (Wu *et al.*, 2011). Theoretically, based on a cis-acting association, this consideration would further increase the binding affinity of ESCRT-0 for ubiquitin, enabling cargo clustering, which is observed *in vivo*.

The architecture of the ESCRT-0 complex has been studied extensively. From cell extracts, Hrs and STAM co-purify in stoichiometric quantities, suggesting that they associate constitutively (Ren *et al.*, 2009). In addition, when co-expressed recombinantly, the proteins form an elongated 1:1 heterodimeric complex (Mayers *et al.*, 2011; Ren *et al.*, 2009). The interface between the subunits has been resolved crystallographically and is composed of two domain-swapped GAT domains that are connected by an antiparallel coiled-coil (Prag *et al.*, 2007; Ren *et al.*, 2009). Based on molecular dynamics simulations, the intact ESCRT-0 complex exhibits a high degree of flexibility, which would enable its multiple ubiquitin-binding domains to lie in close proximity for cargo capture (Ren *et al.*, 2009). Localization studies indicate that ESCRT-0 accumulates mostly on early endosomes. This distribution is directed, at least in part, by a FYVE domain within Hrs (Burd & Emr, 1998; Katzmann *et al.*, 2003; Raiborg *et al.*, 2001b), which exhibits nanomolar affinity for the endosomally-enriched phospholipid, phosphatidylinositol 3-phosphate (PI3P) (Stahelin *et al.*, 2002). Mutations in the FYVE domain that abolish PI3P binding result in the cytosolic accumulation of ESCRT-0 (Katzmann *et al.*, 2003; Raiborg *et al.*, 2001b; Urbé *et al.*, 2000). However, when expressed alone, the Hrs FYVE domain is insufficient to target to endosomes, suggesting additional requirements for ESCRT-0 membrane binding (Gillooly *et al.*, 2000; Raiborg *et al.*, 2001b)

Two crystal structures for the Hrs FYVE domain have been solved. While the yeast protein fragment is monomeric (Misra & Hurley, 1999), the structure obtained using Drosophila Hrs, which includes both the FYVE and the upstream VHS domains, reveals a potential for dimerization (Mao *et al.*, 2000). In the latter structure, two FYVE domains are oriented in an antiparallel fashion and coordinated by citrate ions, which may mimic PI3P (Mao *et al.*, 2000). When expressed in cells as a tandem dimer, the Hrs FYVE domain targets to endosomes efficiently, similar to the full-length protein (Hayakawa *et al.*, 2004). These data suggest that the formation of an Hrs dimer may be a necessary prerequisite for its endosomal localization. Further support for the existence of an Hrs dimer *in vivo* comes from fluorescence resonance energy transfer (FRET)-based experiments, in which ectopically expressed CFP-Hrs undergoes unquenching upon photobleaching of YFP-Hrs on endosomes (Hayakawa *et al.*, 2004), and from hydrodynamic studies conducted using *Caenorhabditis elegans* embryo extracts (Mayers *et al.*, 2011). To resolve the apparent contradiction between cell-based studies, which support the idea that Hrs exists as a dimer, and *in vitro* studies that argue that Hrs co-assembles with STAM in a 1:1 heterodimer in solution, recombinant ESCRT-0 was visualized on synthetic lipid bilayers using atomic force microscopy. These studies revealed that the Hrs:STAM heterodimer undergoes oligomerization specifically on membranes, generating mostly 2:2 heterotetramers (Mayers *et al.*, 2011). The resulting complex brings together at least 8 low affinity ubiquitin-binding motifs, providing the avidity that is likely required for ubiquitin-dependent cargo sorting *in vivo*. Nonetheless, the minimal number of ubiquitin-binding domains necessary for this process remains unclear, although it is likely that both Hrs and STAM contribute significantly.

The carboxyl-termini of the ESCRT-0 subunits largely function as interaction hubs. The SH3 domains of STAM associate with the DUBs, AMSH and UBPY, which were described earlier (Kato *et al.*, 2000; Tanaka *et al.*, 1999). Additionally, Hrs encodes a clathrin-interaction motif, enabling ESCRT-0 to associate with flat clathrin lattices that assemble on early endosomes (Raiborg *et al.*, 2001a, 2002). These lattices likely facilitate clustering of ESCRT-0 into microdomains, which ultimately define sites of ILV formation. Deletion of the clathrin-binding box in Hrs results

in a more uniform distribution on endosomes, consistent with its role in clustering ESCRT-0 (Raiborg *et al.*, 2001a). However, the interaction between Hrs and clathrin may not be restricted to the endosome. Additional associations with several endocytic adaptors, including the AP-2 and FCHO-Eps15-Intersectin (FEI) complexes, also target ESCRT-0 to clathrin-coated pits at the plasma membrane (Mayers *et al.*, 2013). Although devoid of PI3P, the concentration of anionic phospholipids (e.g. phosphatidylserine) at the plasma membrane is relatively high (Leventis & Grinstein, 2010), which supports membrane association of ESCRT-0, in coordination with multiple protein-protein interactions. Notably, ESCRT-0 localizes to only a small subset of clathrin-coated pits, suggesting that additional regulatory mechanisms control its distribution on the cell surface (Mayers *et al.*, 2013). One attractive possibility is that the concentration of ubiquitin-modified cargoes specifies the set of nascent clathrin-coated vesicles to which ESCRT-0 is recruited, thereby coupling ESCRT function to ubiquitin-mediated signaling during pit maturation (Henry *et al.*, 2012).

Inhibition of ESCRT-0 recruitment to coated pits does not impair the rate of clathrin-mediated endocytosis, but instead slows the progress of ubiquitin-modified cargoes through the endolysosomal system (Mayers *et al.*, 2013). These data support an early role for ESCRT-0 in substrate recognition at the plasma membrane, which facilitates rapid downstream sorting to lysosomes. There is currently no evidence to support an analogous role for ESCRT-0 at the Golgi. Instead, members of the GGA family of clathrin adaptors function in this capacity and engage biosynthetic cargoes through their low affinity ($\sim$180 μM), ubiquitin-binding GAT domains (Bilodeau *et al.*, 2004; Puertollano & Bonifacino, 2004; Scott *et al.*, 2004; Shiba *et al.*, 2004). Each GAT domain is potentially capable of binding two ubiquitin molecules simultaneously, which may facilitate initial cargo recognition and concentration (Bilodeau *et al.*, 2004; Prag *et al.*, 2005). However, the mechanism underlying cargo transfer to the ESCRT machinery at the early endosome remains unclear.

In addition to its role in cargo sorting, ESCRT-0 also acts as a key adaptor for ESCRT-I recruitment to endosomes. Specifically, a PxxP motif within the Hrs carboxyl-terminus associates with a ubiquitin E2 variant (UEV) domain in Tsg101, one of the core ESCRT-I subunits (Bache *et al.*, 2003; Bilodeau *et al.*, 2003; Katzmann *et al.*, 2003; Lu *et al.*, 2003). However, the affinity of this interaction is weak (in the low μM range) and fails to support a constitutive localization of ESCRT-I to endosomal subdomains that contain ESCRT-0 (Ren & Hurley, 2011; Pornillos *et al.*, 2003). Nonetheless, depletion of ESCRT-0 inhibits ESCRT-I recruitment and function, indicating that a clear hierarchical assembly pathway exists for the ESCRT machinery in endosomal sorting (Bache *et al.*, 2003; Katzmann *et al.*, 2003). In species that lack ESCRT-0, including protists and plants, an alternative adaptor regulates ESCRT-I targeting to endosomes. The best candidates for this activity are members of the Tom1 family, which all harbor GAT domains that bind ubiquitin and additional motifs that associate with clathrin, Tsg101, and membrane phospholipids (Blanc *et al.*, 2009; Herman *et al.*, 2011; Shiba *et al.*, 2004; Yamakami *et al.*, 2003; Yanagida-Ishizaki *et al.*, 2008). Tom1 and Tom1-like proteins are more

highly conserved as compared to ESCRT-0, although their function(s) in animal cells have yet to be clearly defined (Seet *et al.*, 2004).

The UEV domain of Tsg101 also binds to ubiquitin (Bilodeau *et al.*, 2003; Katzmann *et al.*, 2001; Pornillos *et al.*, 2002), albeit with poor affinity ($\sim$510 μM), utilizing a region that is distinct from the Hrs interaction motif (Garrus *et al.*, 2001; Sundquist *et al.*, 2004). These data suggest that the ESCRT-I complex may also participate in ubiquitin-dependent cargo sorting. However, a mutation in yeast Tsg101 that inhibits ubiquitin binding fails to affect the transport of several model ESCRT-dependent cargoes (Shields *et al.*, 2009). Biochemical analysis of ESCRT-I has revealed a potential for numerous unique complexes to form in cells. In all cases, four distinct subunits (Tsg101, Vps28, a Vps37 isoform, and a Mvb12 or UBAP1 isoform) co-assemble with a 1:1:1:1 stoichiometry to generate a heterotetramer in solution (Agromayor *et al.*, 2012; Audhya *et al.*, 2007; Kostelansky *et al.*, 2007; Morita *et al.*, 2007a) (Figure 2). Crystallographic and small-angle X-ray scattering (SAXS) studies focusing on yeast ESCRT-I indicate that the complex is elongated ($\sim$22.5 nm) with highly flexible termini that can engage ESCRT-0 and ESCRT-II, respectively (Boura *et al.*, 2011;
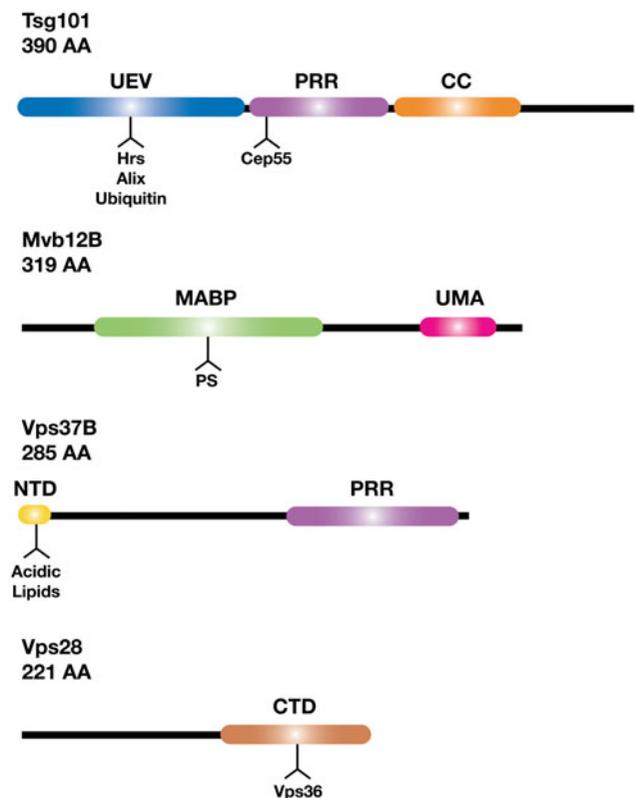
Figure 2. Domain organization of widely conserved ESCRT-I subunits. Illustrations highlight the key domains within the ESCRT-I subunits and their interacting partners. In mammals, four isoforms of Vps37 are expressed (Vps37A, Vps37B, Vps37C and Vps37D). Additionally, there are two distinct Mvb12 subunits (Mvb12A and Mvb12B) or a single UBAP1 isoform that can co-assemble with Tsg101, Vps28 and one Vps37 subunit. Abbreviations: Coiled-Coil (CC), C-Terminal Domain (CTD), Mvb12-associated β-prism (MABP), N-Terminal Domain (NTD), Phosphatidylserine (PS), Proline Rich Region (PRR), Ubiquitin E2 variant (UEV), Ubap1-Mvb12-Associated (UMA). (see colour version of this figure at www.informahealthcare.com/bmg).

Kostelansky *et al.*, 2007). However, a structure for metazoan ESCRT-I is lacking.

Although a specific function for human Mvb12 isoforms in endosomal protein sorting has yet to be demonstrated, UBAP1 and yeast Mvb12 have both been shown to bind ubiquitin and affect the kinetics of cargo degradation (Agromayor *et al.*, 2012; Shields *et al.*, 2009; Stefani *et al.*, 2011). The affinity of yeast Mvb12 for ubiquitin has not been determined. However, structural studies place its ubiquitin-binding carboxyl-terminus near the UEV domain of Tsg101, suggesting both domains could bind with elevated avidity to a diubiquitin-modified cargo (Boura *et al.*, 2011; Shields *et al.*, 2009). Isothermal titration calorimetry studies indicate that UBAP1 associates with ubiquitin with low affinity ($\sim$140 μM in the context of an intact ESCRT-I complex), similar to the DUIM of Hrs (Agromayor *et al.*, 2012). A solution structure of the UBAP1 carboxyl-terminus revealed the presence of overlapping ubiquitin associated (UBA) domains, which may engage up to three ubiquitin molecules simultaneously. However, binding studies indicate that the overlapping UBA domains bind equally to monoubiquitin as compared to diubiquitin (Agromayor *et al.*, 2012).

In addition to its ability to associate with ESCRT-0, the ESCRT-I complex also associates weakly with acidic phospholipids, which are enriched on early endosomes (Boura & Hurley, 2012; Kostelansky *et al.*, 2007). In particular, an amino-terminal basic patch in yeast Vps37, which is not conserved in higher eukaryotes (Kostelansky *et al.*, 2007), and the MVB12-associated β-prism (MABP) domain of mammalian Mvb12 isoforms have been shown to bind phosphatidylserine-containing liposomes *in vitro* (Boura & Hurley, 2012). It is possible that additional domains of ESCRT-I also bind membrane phospholipids, but these may be difficult to identify, given the overall poor affinity of ESCRT-I for bilayers. Nonetheless, coincidence detection of ESCRT-0 and acidic phospholipids is likely responsible for directing ESCRT-I to associate transiently with endosomes *in vivo*.

Similar to ESCRT-I, the ESCRT-II complex does not stably associate with endosomes. However, interactions with acidic phospholipids and ESCRT-I enable its temporary recruitment (Teo *et al.*, 2006). Biochemical studies indicate that ESCRT-II forms a stable heterotetramer in solution that is composed of 3 unique subunits: Vps22, Vps36, and two copies of Vps25 (Babst *et al.*, 2002b; Im & Hurley, 2008) (Figure 3). Two of these bind to membranes, including the Gram-like ubiquitin-binding in Eap45 (GLUE) domain in Vps36, which exhibits a minor preference for PI3P and contributes little to ESCRT-II localization (Slagsvold *et al.*, 2005; Teo *et al.*, 2006), and a conserved, basic helical domain in Vps22 that nonspecifically associates with acidic phospholipids, but is required for ESCRT-II endosomal targeting (Im & Hurley, 2008). Although mammalian and yeast Vps36 differ in the organization of their GLUE domains, both can also bind to ubiquitin in a manner that is not competitive with phosphoinositides (Alam *et al.*, 2004; Gill *et al.*, 2007; Slagsvold *et al.*, 2005). Additionally, the yeast GLUE domain contains two Npl4 type zinc fingers, the first of which binds to the carboxyl-terminal domain of the ESCRT-I subunit Vps28 (Gill *et al.*, 2007), while the second binds to ubiquitin
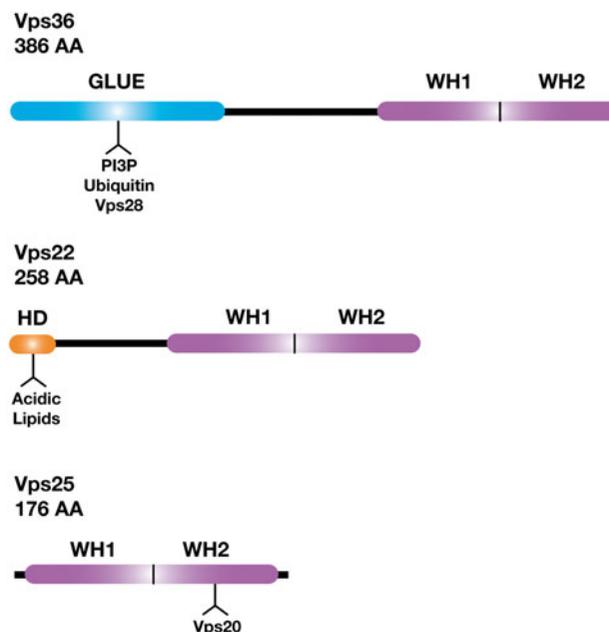

Figure 3. Domain organization of the ESCRT-II subunits. Illustrations highlight the key domains within the ESCRT-II components and their interacting partners. Abbreviations: GRAM-Like Ubiquitin-binding in EAP45 (GLUE), Helical-Domain (HD), Winged-Helix (WH). (see colour version of this figure at www.informahealthcare.com/bmg).
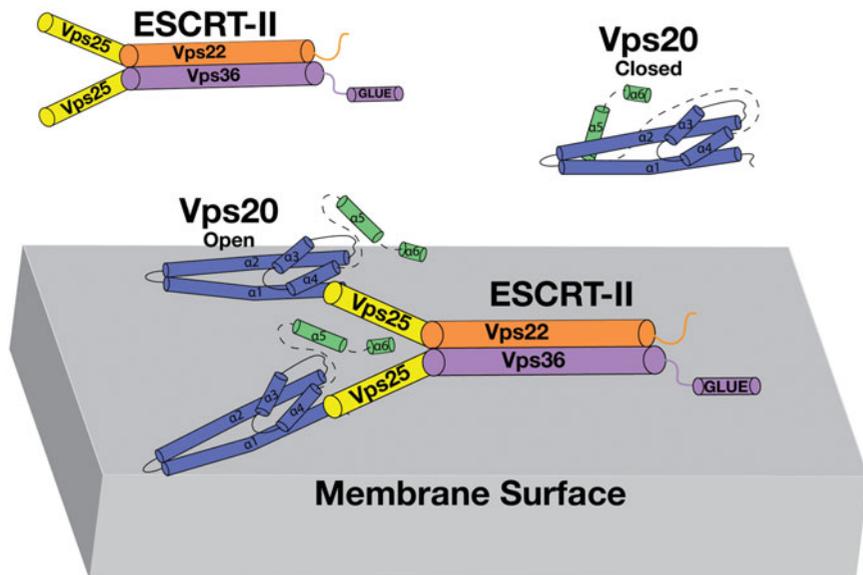
(Alam *et al.*, 2004). Like other ubiquitin-binding domains identified in the early-acting ESCRT machinery, GLUE domains bind to ubiquitin with low affinity ($\sim$330 μM and $\sim$182 μM for mammalian and yeast Vps36 isoforms, respectively) (Alam *et al.*, 2004; Hirano *et al.*, 2006; Slagsvold *et al.*, 2005). It is important to note that irrespective of origin, ESCRT-II complexes contain only a single ubiquitin binding site. Some models suggest that cargo may be transferred from ESCRT-0 to ESCRT-I and/or ESCRT-II. However, mechanistic details to support this possibility have not been identified. Moreover, it is difficult to envision how ubiquitin-modified substrates would be released from ESCRT-0 in favor of binding to downstream ESCRT complexes, as both ESCRT-I and ESCRT-II harbor fewer ubiquitin-binding motifs (with similar or weaker affinities for ubiquitin) and neither stably associates with membranes. Although we cannot rule out the possibility of cargo transfer, a more likely scenario is that ESCRT-0 initially sequesters cargoes into endosomal microdomains, while simultaneously recruiting ESCRT-I and ESCRT-II to further inhibit lateral diffusion of substrates in the membrane. Dissociation of the early-acting complexes is likely coupled to DUB activity, but precisely how cargoes are efficiently deposited into ILVs remains a major outstanding question in the field. Although neither of the late-acting ESCRT complexes encodes cargo-binding motifs, ESCRT-II mediated assembly of ESCRT-III may locally retain cargoes within nascent vesicles until completion of the scission process (Teis *et al.*, 2008; Wollert *et al.*, 2009; Wollert & Hurley, 2010).

ESCRT-mediated membrane bending

In addition to sequestering ubiquitin-modified cargoes, the ESCRT machinery must also induce curvature at the

RIGHTS LINK<)

endosome limiting membrane to drive intralumenal vesicle formation. Both early- and late-acting components have been proposed to function in this capacity, and the field has yet to reach a consensus on the division of labor. Based on *in vitro* studies using giant unilamellar vesicles (GUVs) and purified yeast proteins, a combination of ESCRT-I and ESCRT-II were shown to generate inward budding structures that were several microns in diameter (Wollert & Hurley, 2010). However, for several reasons, the physiological relevance of these findings has been called into question. First, recombinant forms of yeast ESCRT-I and ESCRT-II bind avidly in solution with nanomolar affinity (Gill *et al.*, 2007), a finding that contradicts studies using native forms of the complexes, which do not bind in yeast cell extracts (Babst *et al.*, 2002b; Katzmann *et al.*, 2001). Thus, key regulatory controls are absent in the studies that take advantage of these recombinant yeast complexes, complicating the interpretation of their membrane bending capabilities. Second, the binding interface between yeast ESCRT-I and ESCRT-II is not conserved in metazoan or plant systems, indicating that these complexes associate in a distinct (and yet to be fully defined) manner outside of fungi. Consistent with this idea, recombinant forms of *C. elegans* ESCRT-I and ESCRT-II do not bind with nanomolar affinity in solution nor on membranes, and incubation of these complexes with GUVs fails to induce bud formation above protein-free controls (our unpublished data). Additionally, incubation of human ESCRT-I and ESCRT-II with GUVs does not result in the formation of inward buds (Carlson & Hurley, 2012). Third, the size of nascent vesicles formed in the presence of recombinant yeast ESCRT-I and ESCRT-II (Wollert & Hurley, 2010) are two orders of magnitude larger than those expected, based on the average diameter of native ILVs (~25 nm in yeast) (Richter *et al.*, 2007). A basis for this discrepancy is unclear, but could suggest that the membrane binding of the yeast ESCRT complexes stabilizes spontaneous deformations that occur on GUVs and promotes the formation of internal vesicles. Notably, the size of spontaneously formed vesicles within GUVs is similar to that observed upon addition of the yeast ESCRT machinery (Fyfe *et al.*, 2011; Wollert *et al.*, 2009).

An alternative model suggests a more direct role for the late-acting ESCRT machinery in generating membrane curvature on endosomes. In contrast to the early-acting complexes, ESCRT-III assembly occurs only on lipid bilayers *in vivo* (Babst *et al.*, 2002a). The core ESCRT-III components, as defined in yeast, include Vps20, Vps32, Vps24 and Vps2, which are recruited sequentially (Teis *et al.*, 2008). In addition, metazoan isoforms of Did2, Vps60, Ist1 and CHMP7 each play important, non-redundant roles in ESCRT-III function (Howard *et al.*, 2001; Horii *et al.*, 2006; Shim *et al.*, 2006; Ward *et al.*, 2005). The initial recruitment of Vps20 to endosomes is mediated by the Vps25 subunits of ESCRT-II, which exhibits a Y-shaped architecture based on crystallography studies (Hierro *et al.*, 2004; Im & Hurley, 2008; Teo *et al.*, 2004) (Figure 4). The two copies of Vps25 form distinct lobes that extend away from a third region that is formed by a heterodimer of Vps22 and Vps36. The ends of the Vps25 subunits in the complex possess exposed hydrophobic patches that bind directly to Vps20, likely in a conserved manner (Teo *et al.*, 2004). Mutational analysis indicates that both copies of Vps25 are required for cargo sorting *in vivo*, suggesting that the nucleation of multiple ESCRT-III complexes by ESCRT-II is essential for function (Hierro *et al.*, 2004; Teis *et al.*, 2010).

All ESCRT-III proteins possess a similar domain organization, which includes a basic amino-terminus composed of two alpha helices and an acidic carboxyl-terminus harboring at least an additional three alpha helices. Fragments of three ESCRT-III subunits have been resolved by X-ray crystallography (Figure 5). These studies demonstrate that the basic helices of human Vps32 (hVps32), human Vps24 (hVps24), and Ist1 exhibit extensive similarity, forming a ~7 nm helical hairpin (Bajorek *et al.*, 2009; Lata *et al.*, 2008a; Martinelli *et al.*, 2012; Muzioł *et al.*, 2006). Additionally, the structure of hVps24 derived from residues 9–183 revealed that the adjacent helices (α3 and α4) pack against the open end of the helical hairpin asymmetrically to generate a four-helix bundle (Muzioł *et al.*, 2006). The fifth helix (α5) is connected to the rest of hVps24 by a disordered linker of ~20 amino acids. The analogous region of Ist1 (residues 1–189) exhibits a

Figure 4. ESCRT-II binds to Vps20 to initiate ESCRT-III polymerization. Vps20 is believed to exhibit a closed conformation within the cytoplasm and is unable to interact with ESCRT-II. However, upon recruitment to the endosomal membrane by ESCRT-II, Vps20 autoinhibition is relieved by a mechanism that is currently undefined. (see colour version of this figure at www.informahealthcare.com/bmg).

Figure 5. Overlays of solved ESCRT-III structures. (Top) Representative image from the overlay of the helical hairpin region for human Vps32B (PDB code: 4ABM) and human Vps24 (3FRT). (Middle) Representative image from the overlay of the structures for human Vps24 in the proposed closed (PDB code: 3FRT) and open (PDB code: 2GD5) conformations. (Bottom) Representative image from the overlay of the structures for human Vps24 (PDB code: 3FRT) and human Ist1 (3FRR). (see colour version of this figure at www.informahealth-care.com/bmg).

hVps24 3FRT (Closed)
hVps32B 4ABM
hVps24 2GD5 (Open)
hIst1 3FRR
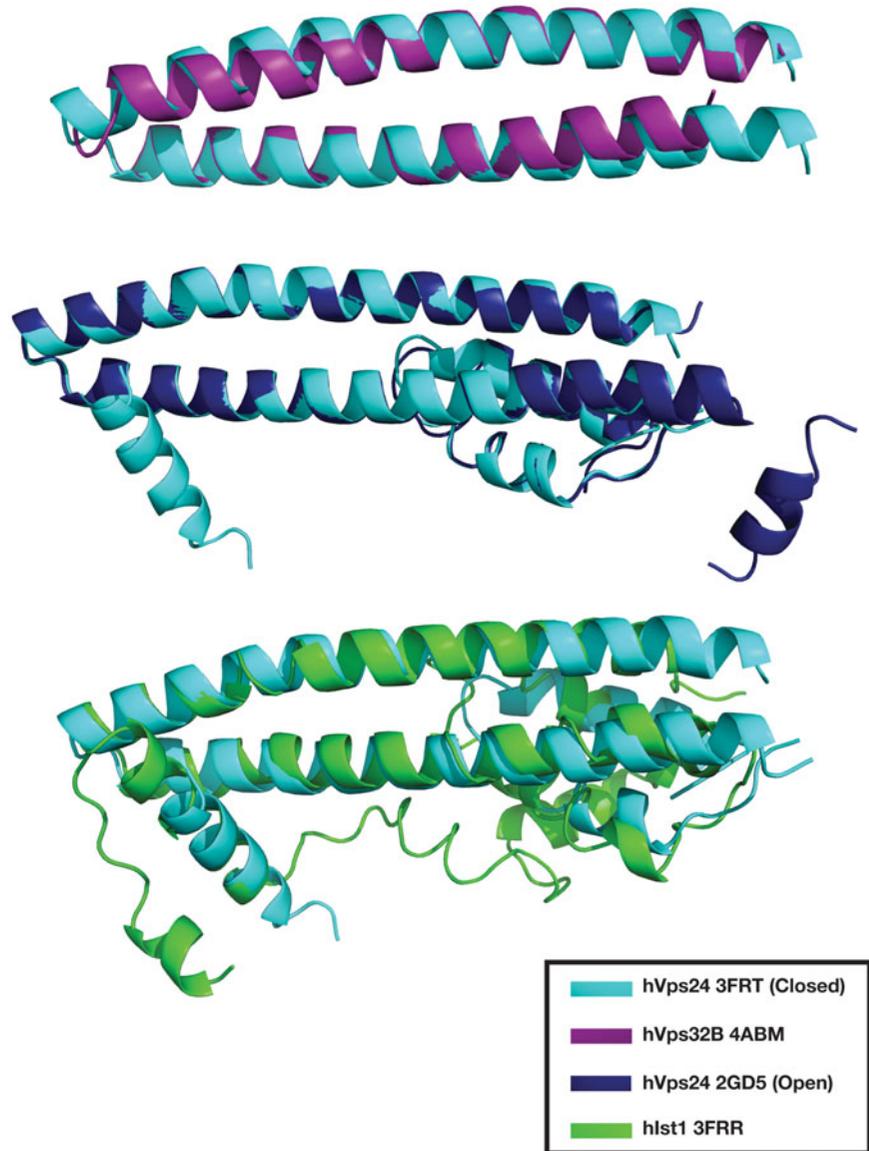
similar architecture with respect to the 4-helix bundle (Bajorek *et al.*, 2009). However, one striking difference between the hVps24 and Ist1 structures is the position of helix 5. In Ist1, this acidic helix packs against the closed end of the hairpin, resulting in a ''closed'' conformation (Bajorek *et al.*, 2009), while the analogous helix in hVps24 fails to contact the helical hairpin, generating an ''open'' conformation (Muzioł *et al.*, 2006). Based on these structures and prediction models, all ESCRT-III subunits are likely to adopt the 4-helix bundle configuration, with a fifth helix connected by a highly flexible linker. In addition, secondary structure prediction algorithms propose the presence of a sixth helix downstream of α5 in most cases (Shim *et al.*, 2007). However, this domain has only been observed in a single Ist1 crystal form, under conditions where it is stabilized by lattice contacts (Bajorek *et al.*, 2009). In the context of other ESCRT-III subunits, the dynamic flexibility of α6 likely prevents its visualization by X-ray crystallography.

Crystallization of hVps24 results in multiple structures with distinct interfaces (Bajorek *et al.*, 2009; Muzioł *et al.*, 2006). Although it remains unclear whether any are physiologically relevant, a ''tip-to-tip'' orientation in which the helical hairpin loops of two monomers associate, has been observed in several crystal forms. This interaction is only feasible if helix 5 is displaced away from the helical hairpin, and together with the Ist1 crystal structure, supports the idea that ESCRT-III monomers can adopt multiple conformations that either promote or restrict dimerization. The closed conformation appears to correlate with an autoinhibited state, in which helix 5 blocks interactions with other ESCRT-III subunits (Bajorek *et al.*, 2009; Lata *et al.*, 2008a). By disrupting this intramolecular interaction, which likely results in the transition to an open conformation, several studies have demonstrated that ESCRT-III subunits become activated and exhibit the tendency to polymerize in an unregulated manner (Bajorek *et al.*, 2009; Henne *et al.*, 2012; Lata *et al.*, 2008b; Muzioł *et al.*, 2006; Teis *et al.*, 2008; Zamborlini *et al.*, 2006). When expressed in cells, these activated forms of ESCRT-III impair the function of the ESCRT machinery, due to their ability to oligomerize even in the absence of upstream stimulation (Bajorek *et al.*, 2009; Dukes *et al.*, 2008; Shim *et al.*, 2007; Zamborlini *et al.*, 2006). Thus, the open

conformation observed in the monomeric hVps24 crystal structure likely represents its activated state.

Numerous ESCRT-III proteins have been shown to polymerize, either on their own or together with another subunit, to generate structures of various sizes and shapes (Bodon *et al.*, 2011; Ghazi-Tabatabai *et al.*, 2008; Hanson *et al.*, 2008; Henne *et al.*, 2012; Lata *et al.*, 2008b; Pires *et al.*, 2009). Wild-type yeast Vps32 exhibits a high degree of heterogeneity, forming sheets, rings and filaments (Ghazi-Tabatabai *et al.*, 2008). However, when mutated to relieve autoinhibition and placed on a lipid monolayer, spiral filaments are observed with a thickness of ∼9 nm (Henne *et al.*, 2012). Further analysis revealed that each filament was composed of two intertwined subfilaments. The physiological relevance of these protofilaments is unclear, as their formation requires relatively high concentrations of purified protein (at least 12.5 µM) (Henne *et al.*, 2012). Additionally, overexpressed human Vps32 forms similar spiral shaped filaments at the cortex of tissue culture cells, but they exhibit a thickness of only ∼5 nm (Hanson *et al.*, 2008). Which of these structures is representative of the native Vps32 polymer remains to be shown.

In contrast to the structures assembled by Vps32, yeast Vps24 forms helical filaments with a diameter of ∼15–20 nm when purified at high concentrations (∼380 µM) (Ghazi-Tabatabai *et al.*, 2008). Similarly, activated forms of human Vps24 and Vps2, generated by truncating their carboxyl-termini, co-assemble to generate ∼40 nm wide helical tubes (Lata *et al.*, 2008b). When combined with liposomes, these truncated proteins drive the formation of ∼50–100 nm wide tubules that narrow and close to form a dome. Similarly, overexpression of human Vps2 drives the formation of tubular protrusions that extend away the cell surface and are often shed into the media (Bodon *et al.*, 2011). These membrane-coated tubules exhibit variability in their diameter (∼70–350 nm), but numerous constrictions are observed (to ∼16 nm in diameter) and the ends of tubes close with a dome-like architecture. Both Ist1 and hDid2 also homo-polymerize to generate helical tubes that are ∼700 nm and ∼230 nm in diameter, respectively (Bajorek *et al.*, 2009). These ESCRT-III proteins have been shown to interact directly and can co-assemble to generate similar helical assemblies. Collectively, these findings demonstrate a clear distinction between the types of polymers generated by Vps32 and the subsequent acting ESCRT-III subunits (Vps24, Vps2, hDid2 and Ist1), suggesting these factors act at unique steps of ESCRT-mediated membrane remodeling.

As described earlier, a complex composed of ESCRT-II and Vps20 initiates polymerization of endosomal ESCRT-III. Biochemical studies using purified yeast proteins suggest that this nucleating supercomplex forms only on lipid bilayers (Henne *et al.*, 2012; Teis *et al.*, 2010). Moreover, ESCRT-II binding promotes a conformational change in Vps20, as measured indirectly using environmentally sensitive dyes, suggesting that it relieves Vps20 autoinhibition and fosters its association with Vps32 (Saksena *et al.*, 2009). An X-ray structure of the ESCRT-II:Vps20 interface has been solved, showing that the binding region on Vps20 is restricted to a region of α1 that is distal to the helical hairpin loop that is predicted to contact α5 in the autoinhibited state

(Im *et al.*, 2009). Based on these findings, it is unclear why the ESCRT-II:Vps20 interaction is restricted to membranes. Moreover, a mechanism underlying the proposed activation of Vps20 by ESCRT-II is difficult to fathom, based on their mode of interaction. Due to these apparent incongruities, an alternative interpretation of the spectroscopic data generated using purified proteins and liposomes may be required. It is important to note that a combination of ESCRT-II and Vps20 binds to liposomes with considerably tighter affinity, as compared to either component alone (Fyfe *et al.*, 2011; Im *et al.*, 2010; Teo *et al.*, 2004). Thus, changes in the spectral properties of Vps20 upon ESCRT-II binding may be a result of this effect, as opposed to a relief in autoinhibition.

In addition to the improved membrane binding affinity exhibited by ESCRT-II:Vps20, the supercomplex exhibits a preference for membranes of elevated curvature (Fyfe *et al.*, 2011). Furthermore, based on liposome binding experiments, the ESCRT-II:Vps20 complex behaves in a mechanosensitive manner, responding to increases in membrane curvature by binding more tightly (Fyfe *et al.*, 2011). These studies raise the possibility that ESCRT-II and Vps20 induce membrane curvature at endosomes. In this scenario, an initial deformation of the limiting membrane, potentially generated through ESCRT-mediated clustering of ubiquitin-modified transmembrane proteins (McMahon & Gallop, 2005), would specify a microdomain to which the ESCRT-II:Vps20 complex would be targeted. Binding to a region of elevated curvature may lead to additional membrane deformation, further increasing the curvature at this site. Ultimately, through this feedforward mechanism, a nascent vesicle could form, but ESCRT-II:Vps20 would be restricted to the curved bud neck. Consistent with this idea, a structural model of the ESCRT-II:Vps20 supercomplex has been suggested to promote negative membrane curvature and docks onto a concave membrane with a radius of curvature similar to that observed in metazoan ILVs (Im *et al.*, 2009). Nevertheless, validation of such a model requires additional testing.

Yet another possibility is that downstream ESCRT-III components coordinately drive membrane invagination to create vesicles that bud away from the cytoplasm. Several studies have shown that Vps32 forms flat spirals and circular arrays on lipid bilayers, both *in vitro* and *in vivo*, which are confined mostly to a single plane (Hanson *et al.*, 2008; Henne *et al.*, 2012). However, these structures can be dramatically remodeled to create three-dimensional coiled helices upon the addition of downstream ESCRT-III subunits (Vps24 and Vps2) or a mutant form of the AAA ATPase Vps4, which cannot hydrolyze ATP (Hanson *et al.*, 2008; Henne *et al.*, 2012). The diameter of the helical tubes that appear when Vps24 and Vps2 are added to pre-existing Vps32 flat spirals is distinct from that observed using truncated forms of Vps24 and Vps2 (∼85 nm versus ∼40 nm, respectively) (Henne *et al.*, 2012; Lata *et al.*, 2008b). These data support the idea that Vps32 spiral filaments transition from a planar arrangement to a more extended conformation, as opposed to nucleating Vps24:Vps2 helices. Such reorganization in Vps32 filaments could result in membrane deformation, although it is unclear how a spherical ILV, shown to be ∼50 nm in diameter in metazoan cells and devoid of internal ESCRT-III, would be generated in this scenario. Based on the

analysis of flat Vps32 spirals that are remodeled in cells though an association with an ATPase deficient form of Vps4, 100–120 nm buds and helical tubes that are scaffolded by ESCRT-III filaments are observed (Hanson *et al.*, 2008). As ESCRT components are not consumed during the process of ILV budding, these structures are unlikely to be related to intermediates in the vesicle budding process *in vivo*. For an analogous reason, membrane deformations generated by Vps24:Vps2 helical tubes also cannot explain the initiation of vesicle formation at endosomes.

ESCRT-mediated membrane scission

The process of vesicle biogenesis concludes with a membrane scission step that results in a complete separation of the donor membrane from the vesicle. There is a wide consensus in the field that the ESCRT-III complex is principally involved in the release of vesicles into the endosome lumen, but the mechanism remains undefined. Deletion of any core ESCRT-III subunit in yeast blocks ILV formation (Babst *et al.*, 2002a). Additionally, using a GUV-based assay, recombinant forms of Vps20, Vps32 and Vps24 have been shown to be sufficient to form large, nascent buds and release them into the GUV lumen, although high concentrations of each factor were necessary to mediate both steps (Wollert *et al.*, 2009). Surprisingly, these studies also indicated that Vps2 and ESCRT-IV were dispensable for membrane scission, suggesting that their major contribution was to recycle ESCRT-III components off the membrane subsequent to their action. An alternative viewpoint argues for a more active role for ESCRT-IV in vesicle release, through its ability to bind, restructure and disassemble ESCRT-III filaments (Hanson *et al.*, 2008; Henne *et al.*, 2012; Saksena *et al.*, 2009). Considering that ESCRT-IV binds to all ESCRT-III subunits, albeit with varying affinities (Azmi *et al.*, 2008; Kieffer *et al.*, 2008; Merrill & Hanson, 2010; Shim *et al.*, 2008; Skalicky *et al.*, 2012; Stuchell-Brereton *et al.*, 2007; Xiao *et al.*, 2008), and encodes the only known enzyme that functions in the ESCRT pathway, its bypass in the context of the GUV-based budding reaction may be a result of the highly artificial nature of the assay, as opposed to an indirect role in membrane scission.

The ESCRT-IV complex is composed of two main subunits, the type I AAA ATPase Vps4 (SKD1 in mammals) and its co-factor Vta1 (LIP5 in mammals) (Azmi *et al.*, 2008; Babst *et al.*, 1998; Xiao *et al.*, 2008; Yang & Hurley, 2010; Yeo *et al.*, 2003; Yu *et al.*, 2008). An amino-terminal MIT domain enables Vps4 to bind to nearly all ESCRT-III subunits with affinities in the low-micromolar range (Kieffer *et al.*, 2008; Shim *et al.*, 2008; Skalicky *et al.*, 2012; Stuchell-Brereton *et al.*, 2007). Thus, polymerized ESCRT-III on membranes acts as a potent recruitment factor. In addition, the Vps4 MIT domain may bind to PI3P in a calcium-dependent manner (Iwaya *et al.*, 2013), which could further contribute to ESCRT-IV recruitment to endosomal membranes. Beyond its MIT domain, Vps4 also harbors large and small ATPase domains, a β-domain, and a carboxyl-terminal helix. Like other AAA ATPases, Vps4 binds to ATP at the interface between the large and small ATPase domains using Walker A/B motifs (Babst *et al.*, 1998; Scott *et al.*, 2005a). In the

absence of nucleotide, Vps4 exists in an equilibrium between monomer and dimer states, neither of which exhibits activity (Babst *et al.*, 1998; Gonciarz *et al.*, 2008; Hartmann *et al.*, 2008; Xiao *et al.*, 2007, 2008). However, upon ATP binding, Vps4 oligomerizes to an active form. Mutating a conserved Walker B glutamate residue to glutamine allows for ATP binding and Vps4 oligomerization, but prevents ATP hydrolysis and complex disassembly (Azmi *et al.*, 2006; Babst *et al.*, 1997; Scott *et al.*, 2005a; Stuchell-Brereton *et al.*, 2007; Whiteheart *et al.*, 1994; Xiao *et al.*, 2007, 2008). Using this mutant isoform, studies have shown that yeast Vps4 assembles into dodecameric or tetradecameric complexes that resemble pairs of stacked rings and share the feature of a central pore, which is required for function (Hartmann *et al.*, 2008; Landsberg *et al.*, 2009; Yu *et al.*, 2008). Models suggest that ESCRT-III subunits contact the pore directly and potentially pass through the stacked ring structure, leading to disassembly of filaments. However, direct evidence in support of these models is lacking. Moreover, recent work examining the oligomeric state of wild-type yeast Vps4 in the presence of ATP contradicts prior studies and indicates that Vps4 self-associates to form mostly hexamers in a concentration-dependent manner, a finding that is consistent with the assembly mode of other Type I AAA ATPases (Monroe *et al.*, 2013; Roll-Mecak & Vale, 2008; Zhang *et al.*, 2000). These data argue that the stacked ring structures that assemble using mutant, ATPase-deficient Vps4 may not be physiologically relevant. Consistent with this idea, archaeal Vps4 also forms hexamers, but typically not higher order oligomers, in the presence of ATP (Monroe *et al.*, 2013). Thus, the mechanism by which Vps4 acts on ESCRT-III complexes may be more similar to that of other Type I AAA ATPases (e.g. spastin) than previously thought.

Vta1 binds directly to Vps4 and has been suggested to potentiate its activity (Azmi *et al.*, 2008; Norgan *et al.*, 2013; Shim *et al.*, 2008) and stabilize its oligomeric conformation (Azmi *et al.*, 2006). This regulatory subunit of ESCRT-IV contains two amino-terminal MIT domains that associate with a subset of ESCRT-III subunits with low micromolar affinity and a carboxyl-terminal VSL domain, which binds to the β-domain of Vps4 (Agromayor *et al.*, 2009; Scott *et al.*, 2005b; Shim *et al.*, 2008; Skalicky *et al.*, 2012; Yang & Hurley, 2010). In isolation, Vta1 forms stable dimers that were suggested to stabilize the dodecameric architecture of ATPase-deficient Vps4 (Azmi *et al.*, 2006). However, more recent data indicate that Vta1 does not alter the stoichiometry of the more native Vps4 hexamer in the presence of ATP (Monroe *et al.*, 2013). Although this finding does not contradict prior work demonstrating that Vta1 stimulates Vps4 ATPase activity, its regulatory mechanism must be significantly more complex than is currently appreciated. Deletion of Vta1 in yeast inhibits the normal trafficking of ubiquitin-modified cargoes in the endolysosomal system, but the effect is not nearly as severe as loss of other ESCRT components (Azmi *et al.*, 2006; Rue *et al.*, 2008; Shiflett *et al.*, 2004). Similarly, depletion of LIP5 impairs receptor downregulation in mammalian cells (Ward *et al.*, 2005). These studies indicate that Vta1-mediated stimulation of Vps4 is important for the kinetics of cargo transport to the lumen of endosomes, potentially by accelerating the rate of

ESCRT-III complex disassembly during membrane scission events. In addition, the Vta1 MIT domains can further direct ESCRT-IV assembly to ESCRT-III containing membrane microdomains.

Vps4 activity is further regulated by its substrate, ESCRT-III. The amino-terminal MIT domain, which forms a three-helix bundle, can independently engage two distinct motifs in ESCRT-III subunits known as MIM1 and MIM2 (Kieffer *et al.*, 2008; Obita *et al.*, 2007; Stuchell-Brereton *et al.*, 2007). Helices 2 and 3 mediate the MIM1 interaction, while helices 1 and 3 form a unique binding pocket to associate with MIM2. Vps24, Vps2 and Did2 harbor only MIM1 motifs, while Vps20 and Vps32 harbor only MIM2 domains in their acidic carboxyl-termini. In contrast, Ist1 and CHMP7 contain both motifs. While yeast Vps4 is stimulated by MIM1 motifs only, all MIM domains (with the addition of ∼50 residues of upstream sequence) activate mammalian Vps4, highlighting a key distinction between the yeast and metazoan ATPases (Azmi *et al.*, 2008; Merrill & Hanson, 2010). *In vitro*, metazoan Vps4 exhibits extremely little activity in the absence of ESCRT-III subunits, indicating that substrate recognition acts as a key spatial and temporal regulator of ESCRT-IV function (Merrill & Hanson, 2010). Deletion of the Vps4 MIT domain and an adjacent linker increases its basal activity, suggesting that this region normally acts in an autoinhibitory fashion (Babst *et al.*, 1998; Merrill & Hanson, 2010). Relief of autoinhibition through interactions with ESCRT-III subunits likely plays a key role in activating Vps4. Additionally, the acidic nature of the ESCRT-III carboxyl-termini appears to be essential for this function, as other highly acidic molecules (e.g. poly-L-glutamic acid) can also increase Vps4 activity independently of ESCRT-III (Merrill & Hanson, 2010). Together, these findings support a model in which MIT–MIM interactions facilitate the positioning of acidic residues near the ATPase domain to alter its rate of ATP hydrolysis, which is necessary to dismantle ESCRT-III polymers. In an analogous manner, the carboxyl-terminal acidic residues in α-tubulin are critical in activating the AAA ATPase spastin, which severs polymerized microtubules (Roll-Mecak & Vale, 2008; White *et al.*, 2007).

To couple ESCRT-III disassembly to membrane scission, the action of ESCRT-IV must be tightly regulated. In this model, the stepwise removal of ESCRT-III subunits from a pre-existing polymer would tighten the circumference of the vesicle bud neck and facilitate closure. Several prerequisites must be satisfied to consider this hypothesis further. First, ESCRT-III should be anchored to the highly curved membrane at the neck of the nascent vesicle. As described previously, a complex of ESCRT-II and Vps20 displays curvature sensitivity, binding more avidly to highly bent lipid bilayers (Fyfe *et al.*, 2011). Moreover, visualization of ESCRT-II:Vps20-nucleated polymers of Vps32 on bilayers with varying degrees of curvature demonstrated that they too exhibit a strong preference for curved membranes (Fyfe *et al.*, 2011). Additionally, Vps24, Vps2, Did2 and Ist1 are all capable of assembling to helical complexes that deform membranes into tubes of high curvature (Bajorek *et al.*, 2009; Bodon *et al.*, 2011; Lata *et al.*, 2008b). A basis for ESCRT-III membrane binding comes from their three-dimensional structures (solved or modeled), which exhibit electrostatic patches in their common asymmetric 4-helix bundles (Buchkovich *et al.*, 2013). These basic regions, largely found in helices 1, 2 and/or 3, are conducive to binding anionic phospholipids, which are enriched on endosomal membranes. Vps20 is also predicted to undergo myristoylation near its amino-terminus, which would further foster its membrane association (Babst *et al.*, 2002a). More recently, several ESCRT-III subunits have been proposed to contain an amino-terminal motif that can insert into membranes (Buchkovich *et al.*, 2013). Although their depths of penetration have yet to be characterized, spectroscopic measurements suggest that yeast Vps32 can delve partially into bilayers, which would induce membrane curvature. These findings collectively support the idea that ESCRT-III adheres tightly to curved membranes.

Second, ESCRT-IV activity should result in constriction of ESCRT-III polymers as they disassemble to bring opposing membranes in the vesicle bud neck closer together. Relatively few studies have directly examined ESCRT-III remodeling in the presence of active ESCRT-IV. Electron microscopy-based studies indicate that Vps4 binds to the inside of helical tubes composed Vps24 and Vps2 in the absence of ATP and drives their disassembly when ATP is added (Lata *et al.*, 2008a). However, these findings did not clarify the mechanism by which Vps4 alters the helical organization of Vps24:Vps2 polymers that results in disassociation. In cells, Vps32 filaments that assemble upon overexpression bind to an ATPase-deficient form of Vps4 along their entire length (Hanson *et al.*, 2008). In this case, Vps4 binding results in the compaction of Vps32 circular arrays, which is consistent with an active role for ESCRT-IV in reorganizing ESCRT-III architecture, but uncouples the disassembly reaction from constriction. Together, these findings suggest that the current model for ESCRT-IV driven membrane scission requires revision. Instead of acting in a single reaction, ESCRT-IV may function in multiple steps. In an initial binding reaction, ESCRT-III locally concentrates ESCRT-IV, driving its oligomerization into hexameric ring structures. Coupled to this process, ESCRT-IV promotes the constriction of ESCRT-III spiral filaments. In this manner, the opposing membranes in a vesicle bud neck could be brought into close proximity. Finally, interactions between ESCRT-III MIM domains and Vps4 MIT domains allow the acidic motifs in ESCRT-III subunits to activate the Vps4 ATPase, driving disassembly of ESCRT-III polymers, and simultaneously releasing energy to facilitate membrane scission.

An alternative to this model is a more direct role for Vps24:Vps2 in promoting membrane constriction. Based on the architecture of the ends of helical tubes generated by recombinant Vps24 and Vps2, several in the field speculate the these dome-like structures promote membrane sealing during ILV budding (Lata *et al.*, 2008b). Indeed, assembly of such a dome at the vesicle bud neck could draw opposing membranes together to facilitate scission (Elia *et al.*, 2012; Fabrikant *et al.*, 2009). Additionally, based on the hierarchy of ESCRT-III filament assembly, Vps24 and Vps2 are recruited by Vps32, allowing them to act late in the vesicle formation process (Teis *et al.*, 2008). With such a role as is proposed for Vps24:Vps2, ESCRT-IV activity becomes less relevant to scission, although it continues to be required for ESCRT-III
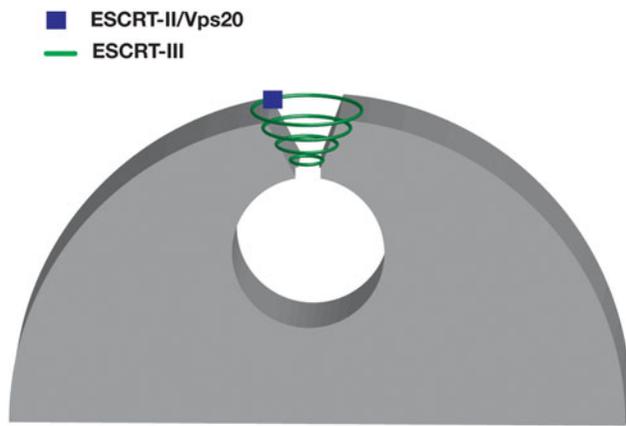
■ ESCRT-II/Vps20
— ESCRT-III

Figure 6. A model for ESCRT-III mediated membrane scission during intralumenal vesicle formation at endosomes. ESCRT-II and Vps20 nucleate ESCRT-III assembly, which narrows the diameter of the vesicle bud neck to facilitate scission. (see colour version of this figure at www.informahealthcare.com/bmg).

disassembly and subunit recycling. Detection of dome-like structures composed of Vps24 and Vps2 have yet to be identified in a native setting, raising concerns about this model. However, their existence may be extremely transient, impeding progress toward their visualization.

It is also feasible that the mechanism of membrane scission requires elements from multiple models (Figure 6). As the initial curvature sensor in the ESCRT machinery, a complex of ESCRT-II and Vps20 may serve to induce membrane bending and vesicle formation at sites where ESCRT-0 has clustered ubiquitin-modified cargoes. Although the mechanism by which Vps32 polymerization is triggered by ESCRT-II:Vps20 remains unclear, it may require a specific conformation of Vps20 that is obtained when the membrane is appropriately bent. Consistent with this idea, ESCRT-II:Vps20 can nucleate Vps32 polymers on areas of high curvature, but not on flat membranes (Fyfe *et al.*, 2011). Cargo diffusion would be restricted by the formation of Vps32 spiral filaments, potentially in a manner akin to that of septin filaments, which create a membrane diffusion barrier between mother and daughter cells in yeast (Hu *et al.*, 2010). Additionally, Vps32 has been shown to recruit DUB enzymes in yeast, which would recycle ubiquitin present on cargo molecules (Ali *et al.*, 2013). The mechanism by which Vps24 binds to Vps32 polymers is unclear. However, their association results in remodeling of Vps32 spiral filaments, which may cause their further penetration into the bud neck (Henne *et al.*, 2012). Additionally, Vps24 has been shown to recruit AMSH in mammalian cells, further supporting cargo deubiquitination (Agromayor & Martin-Serrano, 2006; Kyuuma *et al.*, 2007; Ma *et al.*, 2007; McCullough *et al.*, 2006; Solomons *et al.*, 2011; Tsang *et al.*, 2006; Zamborlini *et al.*, 2006). Formation of a Vps24:Vps20 dome-like structure within the neck would reorganize the membranes, bringing opposing bilayers together within the neck. The final action of ESCRT-IV would further restructure spiral helices within the neck and facilitate spontaneous scission, but only when the membranes there are properly juxtaposed. Further contributions to this set of reactions by the other ESCRT-III components (Ist1, Did2 and Vps60), all of which can

modulate Vps4 ATPase activity (Azmi *et al.*, 2008; Dimaano *et al.*, 2008; Rue *et al.*, 2008; Merrill & Hanson, 2010; Nickerson *et al.*, 2010), would promote scission and subsequent recycling of ESCRT-III subunits after membrane resealing. In particular, the stepwise co-assembly of ESCRT-III subunits would progressively generate a high avidity binding site for ESCRT-IV, both temporally and spatially regulating its action.

ESCRT function during cytokinetic abscission

Cytokinesis is the process that divides two daughter cells from one another after the completion of mitosis. In animal cells, an actin-myosin ring constricts the plasma membrane to create a thin (∼200 nm) intracellular bridge, which must ultimately be resolved by a membrane scission step (Adams *et al.*, 1998; Green *et al.*, 2013; Madaule *et al.*, 1998). Within this structure resides the midbody, which assembles from tightly packed antiparallel microtubules that initially contributed to chromosome segregation (Hu *et al.*, 2012; Mullins & McIntosh, 1982; Saxton & McIntosh, 1987), and the midbody ring, which consists of contractile ring components, including actin and myosin (Breckler & Burnside, 1994; Pohl & Jentsch, 2008; Sanger *et al.*, 1989). In contrast to ILV formation at endosomes, the requirement for the ESCRT machinery to induce membrane curvature is bypassed during abscission. By comparing the set of ESCRT components required for these processes, several conspicuous differences are elucidated. First, ESCRT-0 does not function during cytokinesis, as cargo clustering is not required. However, since ESCRT-I associates weakly and nonspecifically with membranes, a distinct adaptor must exist to localize it and downstream components of the ESCRT machinery appropriately. In mammalian cells, the microtubule bundling protein Cep55 has been shown to bind directly to the Tsg101 subunit of ESCRT-I, enabling it to accumulate at the midbody (Carlton & Martin-Serrano, 2007; Morita *et al.*, 2007b). However, Cep55 is vertebrate-specific, indicating that another factor must exist to mediate ESCRT-I recruitment to the midbody in other metazoans. Consistent with this idea, studies in *C. elegans* have demonstrated that ESCRT-I accumulates at midbodies during embryo development (Green *et al.*, 2013), even though the GPPX$_3$Y motif in human Tsg101 that binds to Cep55 (Lee *et al.*, 2008) is absent in *C. elegans* Tsg101. Additionally, depletion studies show that a small percentage of mammalian cells depleted of Cep55 (∼10–30%) can continue to undergo cell division (Carlton & Martin-Serrano, 2007; Morita *et al.*, 2007b). Thus, an alternative mechanism to recruit ESCRT-I to the midbody exists and may be functionally conserved in all eukaryotes.

Although ESCRT-I participates in both ILV formation and abscission, depletion of its binding partner ESCRT-II does not block cell division (Langelier *et al.*, 2006; Malerød *et al.*, 2007). Additionally, localization studies have failed to show that components of ESCRT-II accumulate at the midbody during cytokinesis. One potential reason for its absence at the midbody is the low levels of PI3P at this site, which normally plays a role in ESCRT-II membrane association on endosomes (Gillooly *et al.*, 2000; Slagsvold *et al.*, 2005). Additionally, depletion of the Vps20 subunit of ESCRT-III

results in very few multinucleated cells, as compared to the depletion of other ESCRT-III activities (Morita *et al.*, 2010). Notably, unlike most ESCRT-III subunits in human cells, Vps20 function is contributed by a single isoform. Thus, if its functions were important during abscission, as appears to be the case for all other ESCRT-III components (Morita *et al.*, 2010), one would anticipate a significant increase in cell division defects upon its loss. Also, without its upstream binding partner ESCRT-II, it is unclear how Vps20 would localize to the midbody, especially given its weak affinity for membranes in isolation (Fyfe *et al.*, 2011; Teo *et al.*, 2004). Perhaps it is not surprising that ESCRT-II and Vps20 are not required in abscission, as their major role in ILV formation may rely mostly on their ability to induce the initial stages of membrane bending, a function that is unnecessary in the context of actin-myosin driven abscission.

In contrast to the dispensable functions of ESCRT-0, ESCRT-II and Vps20 in cytokinesis, some ESCRT components appear to have more significant roles in this process as compared to ILV biogenesis. In particular, depletion of the late-acting ESCRT-III subunits Ist1 and Did2 results in a substantial increase in multinucleated cells, indicatory of a defect in cytokinesis (Agromayor *et al.*, 2009; Bajorek *et al.*, 2009; Morita *et al.*, 2010). However, mutations in these components were not isolated in the original genetic screens that identified the majority of ESCRT components in yeast (Raymond *et al.*, 1992). Moreover, deletion of Ist1 or Did2 individually does not cause a class ''E'' phenotype, indicating a more limited role in ILV biogenesis (Rue *et al.*, 2008). These data suggest that the helical polymers generated by Ist1 and Did2 may function in a more abscission-centric manner, potentially facilitating recruitment of ESCRT-IV in a manner that is not required during ILV scission. Similarly, deletion of Alix, an accessory component of the ESCRT machinery, results in a very weak class ''E'' phenotype in yeast, but its inhibition in human cells causes a dramatic defect in cytokinesis (Carlton & Martin-Serrano, 2007; Carlton *et al.*, 2008; Morita *et al.*, 2007b; Raymond *et al.*, 1992). Alix binds to both Tsg101 (Martin-Serrano *et al.*, 2003; von Schwedler *et al.*, 2003) and Vps32 (McCullough *et al.*, 2008; Pires *et al.*, 2009), raising the possibility that it bridges ESCRT-I and ESCRT-III and enables bypass of ESCRT-II during midbody resolution. However, *in vitro* reconstitution experiments have failed to demonstrate that ESCRT-I and Alix can promote assembly of ESCRT-III polymers (Carlson & Hurley, 2012). Thus, it remains unclear how ESCRT-III filament assembly is initiated within intracellular bridges.

Another key difference between ILV formation and abscission is the timescale of the reactions. While ILVs are generated on the order of seconds to minutes, resolution of the midbody in mammalian tissue culture cells requires ∼1–3 hours or more (reviewed extensively in Barr & Gruneberg, 2007; Eggert *et al.*, 2006; Steigemann & Gerlich, 2009). The dynamics of the ESCRT machinery and its key adaptor during cytokinesis have been studied intensely. Cep55 localizes to centrosomes prior to mitosis and is then distributed onto the mitotic spindle and the spindle midzone microtubules, before it accumulates at the midbody as cells divide (Zhao *et al.*, 2006). During interphase, ESCRT-I accumulates with Cep55 at centrosomes (Morita *et al.*, 2007b, 2010; Xie *et al.*, 1998).

In contrast, detectable levels of ESCRT-I appear at the midbody well after Cep55 has been targeted to the site (Elia *et al.*, 2011). Super resolution-based imaging of ESCRT-I places it at the cortical surface of the midbody, organized in two hollow rings that adhere to the inner leaflet of the plasma membrane (Elia *et al.*, 2011). Alix, which also binds to Cep55, is distributed in a similar manner (Elia *et al.*, 2011; Morita *et al.*, 2007b). These data are consistent with a role for Cep55 in recruitment of the ESCRT machinery, although their limited overlap suggests additional regulation of ESCRT-I distribution, potentially by components of the midbody ring. Assembly of Vps32 occurs subsequently to ESCRT-I arrival, in similar membrane-associated rings, which only partially overlap with ESCRT-I containing structures (Elia *et al.*, 2011). Between 15 and 20 minutes prior to membrane scission, a second population of Vps32 appears ∼1 μm away from the midbody, which marks the site of abscission and exhibits additional constriction relative to the remaining intracellular bridge. An equivalent accumulation of Vps32 occurs on the opposite side of the midbody, although its appearance is not simultaneous with the first event (Lafaurie-Janvore *et al.*, 2013; Elia *et al.*, 2011). In a similar manner, several other ESCRT-III subunits function near the midbody during this time period, including Vps24, Vps2, Ist1 and Did2 (Dukes *et al.*, 2008; Morita *et al.*, 2010). In particular, the Did2 MIM domain has been shown to bind to the MIT domain of spastin, which cleaves microtubules within the intracellular bridge to facilitate membrane scission (Roll-Mecak & Vale, 2008; Yang *et al.*, 2008). The appearance of Vps4, ∼10 minutes prior to each scission event, coincides with the release of the midbody on one side, followed by the other (Elia *et al.*, 2011; Morita *et al.*, 2010). In many cases, the midbody ring is internalized by one of the daughter cells and ultimately degraded within lysosomes (Kuo *et al.*, 2011; Pohl & Jentsch, 2008). Thus, in many respects, the midbody represents an atypical cargo of the ESCRT pathway.

Mechanisms by which the multiple distinct Vps32 populations arise during abscission are unclear. As physical links between these accumulations have been difficult to resolve, it is not yet known whether ESCRT-I and/or Alix could directly initiate ESCRT-III polymerization at constriction sites. Based on tomographic reconstruction of the intracellular bridge in mammalian tissue culture cells, 17 nm thick spiral filaments have been observed near sites of constriction that are adjacent to the midbody (Guizetti *et al.*, 2011). However, the composition of these structures is unknown. As discussed earlier, Vps32 filaments generated *in vivo* and *in vitro* range in diameter from ∼5 nm to ∼9 nm, respectively (Hanson *et al.*, 2008; Henne *et al.*, 2012). Thus, the spirals visualized by tomography are unlikely to correspond to Vps32 filaments, unless they laterally associate or interact with other protein polymers. Alternatively, the spirals could correspond to distinct ESCRT-III polymers, which have been shown to form helical tubes and may be nucleated by Vps32 (Bajorek *et al.*, 2009; Bodon *et al.*, 2011; Lata *et al.*, 2008b) (Figure 7). It is also important to emphasize that several other factors implicated in cytokinesis can form filaments that bind to membranes, including the septin family of proteins (Field *et al.*, 1996; Lukoyanova *et al.*, 2008). Notably, depletion of Septin 9 results in a defect in abscission that is similar to that
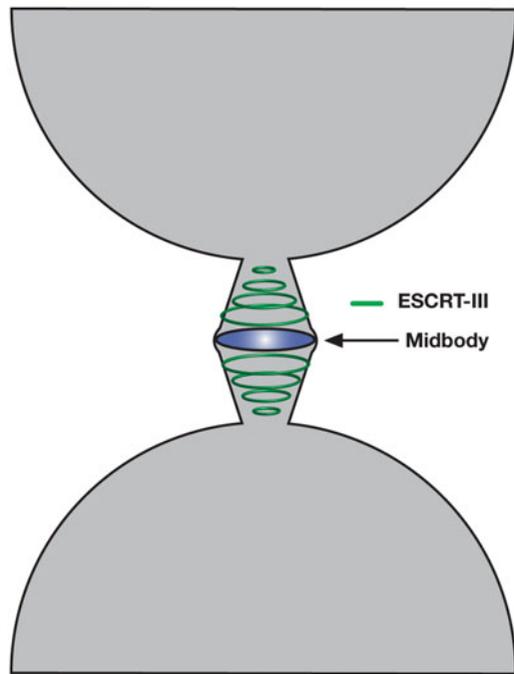
Figure 7. A model for ESCRT-III mediated membrane scission during cytokinetic abscission. Polymerization of ESCRT-III through an unknown mechanism leads to membrane constriction adjacent to the midbody, which facilitates scission of the intracellular bridge and daughter cell separation. (see colour version of this figure at www.informahealthcare.com/bmg).

observed following inhibition of ESCRT-III (Estey *et al.*, 2010). Direct interactions between ESCRT components and septins have not been described. However, the associations may be tightly regulated or require several contact points between multiple subunits to co-assemble. The precise composition of the spiral filaments that form at constriction sites will need to be deciphered to understand their contribution to abscission.

In contrast to other ESCRT-dependent scission events, in which the arrival of ESCRT-III and the ATPase complex coincides with the rapid completion of membrane remodeling, cytokinetic abscission occurs ∼10–20 minutes after the accumulation of ESCRT-III and ESCRT-IV within the intracellular bridge (Elia *et al.*, 2011). These data suggest that regulatory checkpoints that ensure the faithful completion of cytokinesis may exist. By measuring pulling forces between cells during division, tension was found to regulate the timing of abscission (Lafaurie-Janvore *et al.*, 2013). Only when tension was relieved did the daughter cells become fully isolated. The mechanism by which tension is sensed remains unclear, but may involve the Aurora B kinase. During mitosis, Aurora B-mediated phosphorylation destabilizes connections between microtubules that direct chromosome segregation, and kinetochores, which associate directly with DNA (Liu *et al.*, 2009). In the absence of this tension sensing mechanism, chromosome biorientation fails, resulting in chromosome missegregation and aneuploidy. During abscission, Aurora B has been shown to phosphorylate a paralog of Vps32 called CHMP4C, which redirects its localization to the midbody, where both ESCRT-I and Alix localize (Carlton *et al.*, 2012). Here, phosphorylated CHMP4C inhibits

abscission, potentially by impairing the polymerization of other ESCRT-III subunits. It remains to be shown whether Aurora B responds to membrane tension within the intracellular bridge to regulate CHMP4C activity. However, these findings collectively highlight yet another distinction between ESCRT-mediated membrane scission during cytokinesis and ILV budding.

Concluding perspectives

Although the ESCRT machinery is conserved from archaeal species to humans, numerous adaptations have occurred to enable its function in both endolysosomal protein trafficking and cell division (Table 2). The minimal set of ESCRT proteins that can drive membrane scission includes components of ESCRT-III and ESCRT-IV. The locations to which these components are recruited appear to have evolved separately. In archaea, the unique filament forming protein CdvA plays a key role in recruiting ESCRT-III to enable cell division (Dobro *et al.*, 2013). Although CdvA does not exhibit the ability to constrict, the need for this property is rendered moot, as archaeal cells are typically no more than 1 μm in diameter, which appears to be within the capability of ESCRT-III filaments to taper. Budding yeast failed to evolve a recruitment factor for ESCRT-III at the cell division plane, rendering it dispensable for cytokinesis. However, new adaptors enabled ESCRT-III and ESCRT-IV to function in the sorting of integral membrane proteins. To do so, additional machinery was required to capture these molecules (largely ESCRT-0) and bend the endosomal membrane (potentially ESCRT-II:Vps20) to sequester cargoes away from the cytoplasm, thereby terminating their ability to interact with downstream effectors. In this manner, the ESCRT pathway serves as a key tumor suppression system, restricting constitutive signaling that is often a hallmark of cancer (Li & Cohen, 1996; Thompson *et al.*, 2005; Vaccari & Bilder, 2005). Notably, in cases where the ESCRT machinery is required for viral budding, ESCRT-0, ESCRT-II and Vps20 are all dispensable, as cargo capture and membrane bending are processes driven by virally-encoded factors (Langelier *et al.*, 2006; Morita *et al.*, 2011; Sandrin & Sundquist, 2013; von Schwedler *et al.*, 2003). Although plants evolved similar machinery to sort ubiquitin-modified cargoes in the endolysosomal system, an alternative set of cargo adaptors were developed (e.g. the Tom1 family) as compared to yeast and animal cells. These key evolutionary steps help to define how each component of the ESCRT machinery participates in protein trafficking and cytokinetic abscission.

Given their distinctive ability to facilitate membrane scission in a topologically unique manner as compared to the actions of large and small GTPases implicated in other vesicle budding events, it is perhaps not surprising that the ESCRT machinery is hijacked under several forms of viral infection. Successful budding of enveloped viruses requires a scission event at the plasma membrane, which must either be orchestrated by virally encoded proteins (e.g. influenza encoded M2) or host factors (Morita *et al.*, 2011; Rossman *et al.*, 2010). These observations strongly suggest that additional roles for the ESCRT machinery in other virally-induced membrane remodeling events are likely to be

Table 2. Cellular activities of different ESCRT complexes in a variety of species.

Cellular activity	ESCRT complex implicated	Species observed
Receptor trafficking (e.g. EGFR, Notch receptor, LDL receptor, wingless, frizzled, etc.)	ESCRT-0	*S. cerevisiae, C. elegans, D. melanogaster, H. sapiens*
	ESCRT-I	*A. thaliana, S. cerevisiae, C. elegans, D. melanogaster, H. sapiens*
	ESCRT-II	*S. cerevisiae, C. elegans, D. melanogaster, H. sapiens*
	ESCRT-III	*A. thaliana, S. cerevisiae, C. elegans, D. melanogaster, H. sapiens*
	ESCRT-IV	*A. thaliana, S. cerevisiae, C. elegans, D. melanogaster, H. sapiens*
Cell division (e.g. abscission)	ESCRT-0	Not observed
	ESCRT-I	*A. thaliana, D. melanogaster, H. sapiens*
	ESCRT-II	*D. melanogaster*
	ESCRT-III	*D. melanogaster, H. sapiens, S. acidocaldarius*
	ESCRT-IV	*D. melanogaster, H. sapiens, S. acidocaldarius*
Macroautophagy	ESCRT-0	*C. elegans, H. sapiens*
	ESCRT-I	*D. melanogaster, H. sapiens*
	ESCRT-II	*D. melanogaster, H. sapiens*
	ESCRT-III	*A. thaliana, C. elegans, D. melanogaster, H. sapiens*
	ESCRT-IV	*D. melanogaster, H. sapiens*

Although the function of the ESCRT machinery is largely conserved, the roles of the ESCRT complexes in different species vary, which is summarized here. Studies using *S. cerevisiae* (budding yeast), *C. elegans* (nematodes), *D. melanogaster* (insects), *H. sapiens* (human cells), *S. acidocaldarius* (archaea), and *A. thaliana* (plants) are described. Please refer to the text for references.

discovered in the future. Additionally, over the past decade, evidence has mounted that the ESCRT machinery may also function in the process of macroautophagy, in which a double membrane autophagosome engulfs portions of the cytoplasm for lysosome-mediated degradation (reviewed in (Rusten *et al.*, 2012). Closure of the phagophore that is needed to generate a sealed autophagosome requires membrane remodeling that is topologically similar to processes coordinated by the ESCRT machinery. Evidence supporting a direct role for the ESCRT machinery in this pathway is currently lacking, and deletion of yeast ESCRT components do not

inhibit the macroautophagy pathway (Jones *et al.*, 2012). However, the development of new assays or reconstitution-based approaches should resolve this issue in the near future. This area of research is further fueled by the recent implication of the ESCRT machinery in several neurodegenerative diseases, in which mutations in ESCRT components appear to cause defects in autophagy (Lee & Gao, 2009; Lee *et al.*, 2007).

In summary, this review has highlighted the substantial progress made in the ESCRT field over the past several years. However, we have also laid out the major outstanding questions that remain regarding the mechanisms by which the ESCRT machinery acts. By addressing these issues, our understanding of endosomal sorting and cytokinesis will be dramatically improved, and enable a better comprehension of disease states that arise as a result of ESCRT dysfunction.

Declarations of interest

References

Adams RR, Tavares AA, Salzberg A, *et al*. (1998). Pavarotti encodes a kinesin-like protein required to organize the central spindle and contractile ring for cytokinesis. Genes Dev 12:1483–94.

Agromayor M, Carlton JG, Phelan JP, *et al*. (2009). Essential role of hIST1 in cytokinesis. Mol Biol Cell 20:1374–87.

Agromayor M, Martin-Serrano J. (2006). Interaction of AMSH with ESCRT-III and deubiquitination of endosomal cargo. J Biol Chem 281:23083–91.

Agromayor M, Soler N, Caballe A, *et al*. (2012). The UBAP1 subunit of ESCRT-I interacts with ubiquitin via a SOUBA domain. Structure 20: 414–28.

Alam SL, Sun J, Payne M, *et al*. (2004). Ubiquitin interactions of NZF zinc fingers. EMBO J 23:1411–21.

Ali N, Zhang L, Taylor S, *et al*. (2013). Recruitment of UBPY and ESCRT exchange drive HD-PTP-dependent sorting of EGFR to the MVB. Curr Biol 23:453–61.

Amerik AY, Li SJ, Hochstrasser M. (2000). Analysis of the deubiquitinating enzymes of the yeast *Saccharomyces cerevisiae*. Biol Chem 381:981–92.

Amit I, Yakir L, Katz M, *et al*. (2004). Tal, a Tsg101-specific E3 ubiquitin ligase, regulates receptor endocytosis and retrovirus budding. Genes Dev 18:1737–52.

Argenzio E, Bange T, Oldrini B, *et al*. (2011). Proteomic snapshot of the EGF-induced ubiquitin network. Mol Syst Biol 7:462. doi:10.1038/msb.2010.118.

Audhya A, Mcleod IX, Yates JR, Oegema K. (2007). MVB-12, a fourth subunit of metazoan ESCRT-I, functions in receptor downregulation. PLoS One 2:e956.

Azmi I, Davies B, Dimaano C, *et al*. (2006). Recycling of ESCRTs by the AAA-ATPase Vps4 is regulated by a conserved VSL region in Vta1. J Cell Biol 172:705–17.

Azmi IF, Davies BA, Xiao J, *et al*. (2008). ESCRT-III family members stimulate Vps4 ATPase activity directly or via Vta1. Dev Cell 14: 50–61.

Babst M, Katzmann DJ, Estepa-Sabal EJ, *et al*. (2002a). Escrt-III: an endosome-associated heterooligomeric protein complex required for mvb sorting. Dev Cell 3:271–82.

Babst M, Katzmann DJ, Snyder WB, *et al*. (2002b). Endosome-associated complex, ESCRT-Ii, recruits transport machinery for protein sorting at the multivesicular body. Dev Cell 3:283–9.

Babst M, Sato TK, Banta LM, Emr SD. (1997). Endosomal transport function in yeast requires a novel AAA-type ATPase, Vps4p. EMBO J 16:1820–31.

Babst M, Wendland B, Estepa EJ, Emr SD. (1998). The Vps4p AAA ATPase regulates membrane association of a Vps protein

complex required for normal endosome function. EMBO J 17: 2982–93.

Bache KG, Brech A, Mehlum A, Stenmark H. (2003). Hrs regulates multivesicular body formation via ESCRT recruitment to endosomes. J Cell Biol 162:435–42.

Bajorek M, Schubert HL, McCullough J, et al. (2009). Structural basis for ESCRT-III protein autoinhibition. Nat Struct Mol Biol 16: 754–62.

Barr FA, Gruneberg U. (2007). Cytokinesis: placing and making the final cut. Cell 131:847–60.

Bilodeau PS, Winistorfer SC, Allaman MM, et al. (2004). The GAT domains of clathrin-associated GGA proteins have two ubiquitin binding motifs. J Biol Chem 279:54808–16.

Bilodeau PS, Winistorfer SC, Kearney WR, et al. (2003). Vps27-Hse1 and ESCRT-I complexes cooperate to increase efficiency of sorting ubiquitinated proteins at the endosome. J Cell Biol 163:237–43.

Bishop N, Horman A, Woodman P. (2002). Mammalian class E vps proteins recognize ubiquitin and act in the removal of endosomal protein-ubiquitin conjugates. J Cell Biol 157:91–101.

Blanc C, Charette SJ, Mattei S, et al. (2009). Dictyostelium Tom1 participates to an ancestral ESCRT-0 complex. Traffic 10:161–71.

Bodon G, Chassefeyre R, Pernet-Gallay K, et al. (2011). Charged multivesicular body protein 2B (CHMP2B) of the endosomal sorting complex required for transport-III (ESCRT-III) polymerizes into helical structures deforming the plasma membrane. J Biol Chem 286: 40276–86.

Bonifacino JS, Traub LM. (2003). Signals for sorting of transmembrane proteins to endosomes and lysosomes. Annu Rev Biochem 72: 395–447.

Boura E, Hurley JH. (2012). Structural basis for membrane targeting by the MVB12-associated β-prism domain of the human ESCRT-I MVB12 subunit. Proc Natl Acad Sci U S A 109:1901–6.

Boura E, Rózycki B, Herrick DZ, et al. (2011). Solution structure of the ESCRT-I complex by small-angle X-ray scattering, Epr, and FRET spectroscopy. Proc Natl Acad Sci U S A 108:9437–42.

Bowers K, Piper SC, Edeling MA, et al. (2006). Degradation of endocytosed epidermal growth factor and virally ubiquitinated major histocompatibility complex class I is independent of mammalian ESCRTII. J Biol Chem 281:5094–105.

Breckler J, Burnside B. (1994). Myosin I localizes to the midbody region during mammalian cytokinesis. Cell Motil Cytoskeleton 29:312–20.

Buchkovich NJ, Henne WM, Tang S, Emr SD. (2013). Essential N-terminal insertion motif anchors the ESCRT-III filament during MVB vesicle formation. Dev Cell 27:201–14.

Burd CG, Emr SD. (1998). Phosphatidylinositol(3)-phosphate signaling mediated by specific binding to RING FYVE domains. Mol Cell 2: 157–62.

Carlson LA, Hurley JH. (2012). In vitro reconstitution of the ordered assembly of the endosomal sorting complex required for transport at membrane-bound HIV-1 Gag clusters. Proc Natl Acad Sci U S A 109: 16928–33.

Carlton JG, Agromayor M, Martin-Serrano J. (2008). Differential requirements for Alix and ESCRT-III in cytokinesis and HIV-1 release. Proc Natl Acad Sci U S A 105:10541–6.

Carlton JG, Caballe A, Agromayor M, et al. (2012). ESCRT-III governs the Aurora B-mediated abscission checkpoint through CHMP4C. Science 336:220–5.

Carlton JG, Martin-Serrano J. (2007). Parallels between cytokinesis and retroviral budding: a role for the ESCRT machinery. Science 316: 1908–12.

Dimaano C, Jones CB, Hanono A, et al. (2008). Ist1 regulates Vps4 localization and assembly. Mol Biol Cell 19:465–74.

Dobro MJ, Samson RY, Yu Z, et al. (2013). Electron cryotomography of ESCRT assemblies and dividing Sulfolobus cells suggests that spiraling filaments are involved in membrane scission. Mol Biol Cell 24:2319–2327.

Donovan JA, Ota Y, Langdon WY, Samelson LE. (1996). Regulation of the association of p120cbl with Grb2 in Jurkat T cells. J Biol Chem 271:26369–74.

Dukes JD, Richardson JD, Simmons R, Whitley P. (2008). A dominant-negative ESCRT-III protein perturbs cytokinesis and trafficking to lysosomes. Biochem J 411:233–9.

Duncan LM, Piper S, Dodd RB, et al. (2006). Lysine-63-linked ubiquitination is required for endolysosomal degradation of class I molecules. EMBO J 25:1635–45.

Eggert US, Mitchison TJ, Field CM. (2006). Animal cytokinesis: from parts list to mechanisms. Annu Rev Biochem 75:543–66.

Elia N, Fabrikant G, Kozlov MM, Lippincott-Schwartz J. (2012). Computational model of cytokinetic abscission driven by ESCRT-III polymerization and remodeling. Biophys J 102:2309–20.

Elia N, Sougrat R, Spurlin TA, et al. (2011). Dynamics of endosomal sorting complex required for transport (ESCRT) machinery during cytokinesis and its role in abscission. Proc Natl Acad Sci U S A 108: 4846–51.

Ellen AF, Albers SV, Huibers W, et al. (2009). Proteomic analysis of secreted membrane vesicles of archaeal Sulfolobus species reveals the presence of endosome sorting complex components. Extremophiles 13:67–79.

Estey MP, Di Ciano-Oliveira C, Froese CD, et al. (2010). Distinct roles of septins in cytokinesis: SEPT9 mediates midbody abscission. J Cell Biol 191:741–9.

Fabrikant G, Lata S, Riches JD, et al. (2009). Computational model of membrane fission catalyzed by ESCRT-III. PLoS Comput Biol 5: e1000575.

Field CM, AL-Awar O, Rosenblatt J, et al. (1996). A purified Drosophila septin complex forms filaments and exhibits GTPase activity. J Cell Biol 133:605–16.

Fyfe I, Schuh AL, Edwardson JM, Audhya A. (2011). Association of the endosomal sorting complex ESCRT-II with the Vps20 subunit of ESCRT-III generates a curvature-sensitive complex capable of nucleating ESCRT-III filaments. J Biol Chem 286:34262–70.

Garrus JE, von Schwedler UK, Pornillos OW, et al. (2001). Tsg101 and the vacuolar protein sorting pathway are essential for HIV-1 budding. Cell 107:55–65.

Geetha T, Jiang J, Wooten MW. (2005). Lysine 63 polyubiquitination of the nerve growth factor receptor TrkA directs internalization and signaling. Mol Cell 20:301–12.

Ghazi-Tabatabai S, Saksena S, Short JM, et al. (2008). Structure and disassembly of filaments formed by the ESCRT-III subunit Vps24. Structure 16:1345–56.

Gill DJ, Teo H, Sun J, et al. (2007). Structural insight into the ESCRT-I/-II link and its role in MVB trafficking. EMBO J 26:600–12.

Gillooly DJ, Morrow IC, Lindsay M, et al. (2000). Localization of phosphatidylinositol 3-phosphate in yeast and mammalian cells. EMBO J 19:4577–88.

Gonciarz MD, Whitby FG, Eckert DM, et al. (2008). Biochemical and structural studies of yeast Vps4 oligomerization. J Mol Biol 384: 878–95.

Green RA, Mayers JR, Wang S, et al. (2013). The midbody ring scaffolds the abscission machinery in the absence of midbody microtubules. J Cell Biol 203:505–20.

Guizetti J, Schermelleh L, Mäntler J, et al. (2011). Cortical constriction during abscission involves helices of ESCRT-III-dependent filaments. Science 331:1616–20.

Haglund K, Sigismund S, Polo S, et al. (2003). Multiple monoubiquitination of RTKs is sufficient for their endocytosis and degradation. Nat Cell Biol 5:461–6.

Han SO, Kommaddi RP, Shenoy SK. (2013). Distinct roles for β-arrestin2 and arrestin-domain-containing proteins in β2 adrenergic receptor trafficking. EMBO Rep 14:164–71.

Hanson PI, Roth R, Lin Y, Heuser JE. (2008). Plasma membrane deformation by circular arrays of ESCRT-III protein filaments. J Cell Biol 180:389–402.

Hartmann C, Chami M, Zachariae U, et al. (2008). Vacuolar protein sorting: two different functional states of the AAA-ATPase Vps4p. J Mol Biol 377:352–63.

Hayakawa A, Hayes SJ, Lawe DC, et al. (2004). Structural basis for endosomal targeting by FYVE domains. J Biol Chem 279:5958–66.

Henne WM, Buchkovich NJ, Zhao Y, Emr SD. (2012). The endosomal sorting complex ESCRT-II mediates the assembly and architecture of ESCRT-III helices. Cell 151:356–71.

Henry AG, Hislop JN, Grove J, et al. (2012). Regulation of endocytic clathrin dynamics by cargo ubiquitination. Dev Cell 23:519–32.

Herman EK, Walker G, van der Giezen M, Dacks JB. (2011). Multivesicular bodies in the enigmatic amoeboflagellate Breviata anathema and the evolution of ESCRT 0. J Cell Sci 124:613–21.

Herrador A, Herranz S, Lara D, Vincent O. (2010). Recruitment of the ESCRT machinery to a putative seven-transmembrane-domain receptor is mediated by an arrestin-related protein. Mol Cell Biol 30: 897–907.

Hicke L, Dunn R. (2003). Regulation of membrane protein transport by ubiquitin and ubiquitin-binding proteins. Annu Rev Cell Dev Biol 19: 141–72.

Hierro A, Sun J, Rusnak AS, et al. (2004). Structure of the ESCRT-II endosomal trafficking complex. Nature 431:221–5.

Hirano S, Kawasaki M, Ura H, et al. (2006). Double-sided ubiquitin binding of Hrs-UIM in endosomal protein sorting. Nat Struct Mol Biol 13:272–7.

Hoeller D, Crosetto N, Blagoev B, et al. (2006). Regulation of ubiquitin-binding proteins by monoubiquitination. Nat Cell Biol 8: 163–9.

Horii M, Shibata H, Kobayashi R, et al. (2006). CHMP7, a novel ESCRT-III-related protein, associates with CHMP4b and functions in the endosomal sorting pathway. Biochem J 400:23–32.

Howard TL, Stauffer DR, Degnin CR, Hollenberg SM. (2001). CHMP1 functions as a member of a newly defined family of vesicle trafficking proteins. J Cell Sci 114:2395–404.

Hu CK, Coughlin M, Mitchison TJ. (2012). Midbody assembly and its regulation during cytokinesis. Mol Biol Cell 23:1024–34.

Hu Q, Milenkovic L, Jin H, et al. (2010). A septin diffusion barrier at the base of the primary cilium maintains ciliary membrane protein distribution. Science 329:436–9.

Huang F, Kirkpatrick D, Jiang X, et al. (2006). Differential regulation of EGF receptor internalization and degradation by multiubiquitination within the kinase domain. Mol Cell 21:737–48.

Huang F, Zeng X, Kim W, et al. (2013). Lysine 63-linked polyubiquitination is required for EGF receptor degradation. Proc Natl Acad Sci U S A 110:15722–7.

Hurley JH. (2010). The ESCRT complexes. Crit Rev Biochem Mol Biol 45:463–87.

Hurley JH, Emr SD. (2006). The ESCRT complexes: structure and mechanism of a membrane-trafficking network. Annu Rev Biophys Biomol Struct 35:277–98.

Hurley JH, Stenmark H. (2011). Molecular mechanisms of ubiquitin-dependent membrane traffic. Annu Rev Biophys 40:119–42.

Im YJ, Hurley JH. (2008). Integrated structural model and membrane targeting mechanism of the human ESCRT-II complex. Dev Cell 14: 902–13.

Im YJ, Kuo L, Ren X, et al. (2010). Crystallographic and functional analysis of the ESCRT-I /HIV-1 Gag PTAP interaction. Structure 18: 1536–47.

Im YJ, Wollert T, Boura E, Hurley JH. (2009). Structure and function of the ESCRT-II-III interface in multivesicular body biogenesis. Dev Cell 17:234–43.

Iwaya N, Takasu H, Goda N, et al. (2013). MIT domain of Vps4 is a Ca2+-dependent phosphoinositide-binding domain. J Biochem 153: 473–81.

Jiao J, Sun K, Walker WP, et al. (2009). Abnormal regulation of TSG101 in mice with spongiform neurodegeneration. Biochim Biophys Acta 1792:1027–35.

Jones CB, Ott EM, Keener JM, et al. (2012). Regulation of membrane protein degradation by starvation-response pathways. Traffic 13: 468–82.

Kato M, Miyazawa K, Kitamura N. (2000). A deubiquitinating enzyme UBPY interacts with the Src homology 3 domain of Hrs-binding protein via a novel binding motif PX(V/I)(D/N)RXXKP. J Biol Chem 275:37481–7.

Katz M, Shtiegman K, Tal-Or P, et al. (2002). Ligand-independent degradation of epidermal growth factor receptor involves receptor ubiquitylation and Hgs, an adaptor whose ubiquitin-interacting motif targets ubiquitylation by Nedd4. Traffic 3:740–51.

Katzmann DJ, Babst M, Emr SD. (2001). Ubiquitin-dependent sorting into the multivesicular body pathway requires the function of a conserved endosomal protein sorting complex, ESCRT-I. Cell 106: 145–55.

Katzmann DJ, Stefan CJ, Babst M, Emr SD. (2003). Vps27 recruits ESCRT machinery to endosomes during MVB sorting. J Cell Biol 162:413–23.

Kieffer C, Skalicky JJ, Morita E, et al. (2008). Two distinct modes of ESCRT-III recognition are required for VPS4 functions in lysosomal protein targeting and HIV-1 budding. Dev Cell 15:62–73.

Kim BY, Olzmann JA, Barsh GS, et al. (2007). Spongiform neurodegeneration-associated E3 ligase Mahogunin ubiquitylates TSG101 and regulates endosomal trafficking. Mol Biol Cell 18: 1129–42.

Komada M, Soriano P. (1999). Hrs, a FYVE finger protein localized to early endosomes, is implicated in vesicular traffic and required for ventral folding morphogenesis. Genes Dev 13: 1475–85.

Kostelansky MS, Schluter C, Tam YY, et al. (2007). Molecular architecture and functional model of the complete yeast ESCRT-I heterotetramer. Cell 129:485–98.

Kuo TC, Chen CT, Baron D, et al. (2011). Midbody accumulation through evasion of autophagy contributes to cellular reprogramming and tumorigenicity. Nat Cell Biol 13:1214–23.

Kyuuma M, Kikuchi K, Kojima K, et al. (2007). Amsh, an ESCRT-III associated enzyme, deubiquitinates cargo on MVB/late endosomes. Cell Struct Funct 31:159–72.

Kölling R, Hollenberg CP. (1994). The ABC-transporter Ste6 accumulates in the plasma membrane in a ubiquitinated form in endocytosis mutants. EMBO J 13:3261–71.

Lafaurie-Janvore J, Maiuri P, Wang I, et al. (2013). ESCRT-III assembly and cytokinetic abscission are induced by tension release in the intercellular bridge. Science 339:1625–9.

Landsberg MJ, Vajjhala PR, Rothnagel R, et al. (2009). Three-dimensional structure of AAA ATPase Vps4: advancing structural insights into the mechanisms of endosomal sorting and enveloped virus budding. Structure 17:427–37.

Langelier C, von Schwedler UK, Fisher RD, et al. (2006). Human ESCRT-II complex and its role in human immunodeficiency virus type 1 release. J Virol 80:9465–80.

Lata S, Roessle M, Solomons J, et al. (2008a). Structural basis for autoinhibition of ESCRT-III CHMP3. J Mol Biol 378:818–27.

Lata S, Schoehn G, Jain A, et al. (2008b). Helical structures of ESCRT-III are disassembled by VPS4. Science 321:1354–7.

Lee HH, Elia N, Ghirlando R, et al. (2008). Midbody targeting of the ESCRT machinery by a noncanonical coiled coil in CEP55. Science 322:576–80.

Lee JA, Beigneux A, Ahmad ST, et al. (2007). ESCRT-III dysfunction causes autophagosome accumulation and neurodegeneration. Curr Biol 17:1561–7.

Lee JA, Gao FB. (2009). Inhibition of autophagy induction delays neuronal cell loss caused by dysfunctional ESCRT-III in frontotemporal dementia. J Neurosci 29:8506–11.

Leventis PA, Grinstein S. (2010). The distribution and function of phosphatidylserine in cellular membranes. Annu Rev Biophys 39: 407–27.

Levkowitz G, Waterman H, Ettenberg SA, et al. (1999). Ubiquitin ligase activity and tyrosine phosphorylation underlie suppression of growth factor signaling by c-Cbl/Sli-1. Mol Cell 4:1029–40.

Levkowitz G, Waterman H, Zamir E, et al. (1998). c-Cbl/Sli-1 regulates endocytic sorting and ubiquitination of the epidermal growth factor receptor. Genes Dev 12:3663–74.

Li L, Cohen SN. (1996). Tsg101: a novel tumor susceptibility gene isolated by controlled homozygous functional knockout of allelic loci in mammalian cells. Cell 85:319–29.

Lill NL, Douillard P, Awwad RA, et al. (2000). The evolutionarily conserved N-terminal region of Cbl is sufficient to enhance down-regulation of the epidermal growth factor receptor. J Biol Chem 275: 367–77.

Lin CH, Macgurn JA, Chu T, et al. (2008). Arrestin-related ubiquitin-ligase adaptors regulate endocytosis and protein turnover at the cell surface. Cell 135:714–25.

Lindås AC, Karlsson EA, Lindgren MT, et al. (2008). A unique cell division machinery in the Archaea. Proc Natl Acad Sci USA 105: 18942–6.

Liu D, Vader G, Vromans MJ, et al. (2009). Sensing chromosome bi-orientation by spatial separation of aurora B kinase from kinetochore substrates. Science 323:1350–3.

Lu Q, Hope LW, Brasch M, et al. (2003). TSG101 interaction with HRS mediates endosomal trafficking and receptor down-regulation. Proc Natl Acad Sci U S A 100:7626–31.

Lukoyanova N, Baldwin SA, Trinick J. (2008). 3D reconstruction of mammalian septin filaments. J Mol Biol 376:1–7.

Ma YM, Boucrot E, Villén J, et al. (2007). Targeting of AMSH to endosomes is required for epidermal growth factor receptor degradation. J Biol Chem 282:9805–12.

Madaule P, Eda M, Watanabe N, et al. (1998). Role of citron kinase as a target of the small GTPase Rho in cytokinesis. Nature 394:491–4.

Makarova KS, Yutin N, Bell SD, Koonin EV. (2010). Evolution of diverse cell division and vesicle formation systems in Archaea. Nat Rev Microbiol 8:731–41.

Malerød L, Stuffers S, Brech A, Stenmark H. (2007). Vps22/EAP30 in ESCRT-II mediates endosomal sorting of growth factor and chemokine receptors destined for lysosomal degradation. Traffic 8: 1617–29.

Malik R, Marchese A. (2010). Arrestin-2 interacts with the endosomal sorting complex required for transport machinery to modulate endosomal sorting of CXCR4. Mol Biol Cell 21:2529–41.

Mao Y, Nickitenko A, Duan X, et al. (2000). Crystal structure of the VHS and FYVE tandem domains of Hrs, a protein involved in membrane trafficking and signal transduction. Cell 100:447–56.

Marchese A, Raiborg C, Santini F, et al. (2003). The E3 ubiquitin ligase AIP4 mediates ubiquitination and sorting of the G protein-coupled receptor CXCR4. Dev Cell 5:709–22.

Martin-Serrano J, Zang T, Bieniasz PD. (2003). Role of ESCRT-I in retroviral budding. J Virol 77:4794–804.

Martinelli N, Hartlieb B, Usami Y, et al. (2012). CC2D1A is a regulator of ESCRT-III CHMP4B. J Mol Biol 419:75–88.

Mayers JR, Fyfe I, Schuh AL, et al. (2011). ESCRT-0 assembles as a heterotetrameric complex on membranes and binds multiple ubiquitinylated cargoes simultaneously. J Biol Chem 286:9636–45.

Mayers JR, Wang L, Pramanik J, et al. (2013). Regulation of ubiquitin-dependent cargo sorting by multiple endocytic adaptors at the plasma membrane. Proc Natl Acad Sci U S A 110:11857–62.

McCullough J, Clague MJ, Urbé S. (2004). AMSH is an endosome-associated ubiquitin isopeptidase. J Cell Biol 166:487–92.

McCullough J, Colf LA, Sundquist WI. (2013). Membrane fission reactions of the mammalian ESCRT pathway. Annu Rev Biochem 82: 663–92.

McCullough J, Fisher RD, Whitby FG, et al. (2008). ALIX-CHMP4 interactions in the human ESCRT pathway. Proc Natl Acad Sci USA 105:7687–91.

McCullough J, Row PE, Lorenzo O, et al. (2006). Activation of the endosome-associated ubiquitin isopeptidase AMSH by Stam, a component of the multivesicular body-sorting machinery. Curr Biol 16:160–5.

McDonald B, Martin-Serrano J. (2008). Regulation of Tsg101 expression by the steadiness box: a role of Tsg101-associated ligase. Mol Biol Cell 19:754–63.

McMahon HT, Gallop JL. (2005). Membrane curvature and mechanisms of dynamic cell membrane remodelling. Nature 438:590–6.

McMurray MA, Stefan CJ, Wemmer M, et al. (2011). Genetic interactions with mutations affecting septin assembly reveal ESCRT functions in budding yeast cytokinesis. Biol Chem 392:699–712.

Meijer IM, van Leeuwen JE. (2011). ERBB2 is a target for USP8-mediated deubiquitination. Cell Signal 23:458–67.

Meisner H, Czech MP. (1995). Coupling of the proto-oncogene product c-Cbl to the epidermal growth factor receptor. J Biol Chem 270: 25332–5.

Meng B, Lever AM. (2013). Wrapping up the bad news: HIV assembly and release. Retrovirology 10:5. doi:10.1186/1742-4690-10-5.

Merrill SA, Hanson PI. (2010). Activation of human VPS4A by ESCRT-III proteins reveals ability of substrates to relieve enzyme autoinhibition. J Biol Chem 285:35428–38.

Misra S, Hurley JH. (1999). Crystal structure of a phosphatidylinositol 3-phosphate-specific membrane-targeting motif, the FYVE domain of Vps27p. Cell 97:657–66.

Mizuno E, Iura T, Mukai A, et al. (2005). Regulation of epidermal growth factor receptor down-regulation by UBPY-mediated deubiquitination at endosomes. Mol Biol Cell 16:5163–74.

Mizuno E, Kawahata K, Kato M, et al. (2003). STAM proteins bind ubiquitinated proteins on the early endosome via the VHS domain and ubiquitin-interacting motif. Mol Biol Cell 14:3675–89.

Monroe N, Han H, Gonciarz MD, et al. (2013). The oligomeric state of the active Vps4 AAA ATPase. J Mol Biol [Epub ahead of print]. doi: 10.1016/j.jmb.2013.09.043.

Morita E, Colf LA, Karren MA, et al. (2010). Human ESCRT-III and VPS4 proteins are required for centrosome and spindle maintenance. Proc Natl Acad Sci U S A 107:12889–94.

Morita E, Sandrin V, Alam SL, et al. (2007a). Identification of human MVB12 proteins as ESCRT-I subunits that function in HIV budding. Cell Host Microbe 2:41–53.

Morita E, Sandrin V, Chung HY, et al. (2007b). Human ESCRT and ALIX proteins interact with proteins of the midbody and function in cytokinesis. EMBO J 26:4215–27.

Morita E, Sandrin V, McCullough J, et al. (2011). ESCRT-III protein requirements for HIV-1 budding. Cell Host Microbe 9:235–42.

Mullins JM, Mcintosh JR. (1982). Isolation and initial characterization of the mammalian midbody. J Cell Biol 94:654–61.

Muzioł T, Pineda-Molina E, Ravelli RB, et al. (2006). Structural basis for budding by the ESCRT-III factor CHMP3. Dev Cell 10:821–30.

Nickerson DP, West M, Henry R, Odorizzi G. (2010). Regulators of Vps4 ATPase activity at endosomes differentially influence the size and rate of formation of intralumenal vesicles. Mol Biol Cell 21: 1023–32.

Norgan AP, Davies BA, Azmi IF, et al. (2013). Relief of autoinhibition enhances Vta1 activation of Vps4 via the Vps4 stimulatory element. J Biol Chem 288:26147–56.

Obita T, Saksena S, Ghazi-Tabatabai S, et al. (2007). Structural basis for selective recognition of ESCRT-III by the AAA ATPase Vps4. Nature 449:735–9.

Piper RC, Lehner PJ. (2011). Endosomal transport via ubiquitination. Trends Cell Biol 21:647–55.

Pires R, Hartlieb B, Signor L, et al. (2009). A crescent-shaped ALIX dimer targets ESCRT-III CHMP4 filaments. Structure 17:843–56.

Pohl C, Jentsch S. (2008). Final stages of cytokinesis and midbody ring formation are controlled by BRUCE. Cell 132:832–45.

Pornillos O, Alam SL, Rich RL, et al. (2002). Structure and functional interactions of the Tsg101 UEV domain. EMBO J 21:2397–406.

Pornillos O, Higginson DS, Stray KM, et al. (2003). HIV Gag mimics the Tsg101-recruiting activity of the human Hrs protein. J Cell Biol 162: 425–34.

Prag G, Lee S, Mattera R, et al. (2005). Structural mechanism for ubiquitinated-cargo recognition by the Golgi-localized, gamma-ear-containing, ADP-ribosylation-factor-binding proteins. Proc Natl Acad Sci U S A 102:2334–9.

Prag G, Watson H, Kim YC, et al. (2007). The Vps27/Hse1 complex is a GAT domain-based scaffold for ubiquitin-dependent sorting. Dev Cell 12:973–86.

Puertollano R, Bonifacino JS. (2004). Interactions of GGA3 with the ubiquitin sorting machinery. Nat Cell Biol 6:244–51.

Raiborg C, Bache KG, Gillooly DJ, et al. (2002). Hrs sorts ubiquitinated proteins into clathrin-coated microdomains of early endosomes. Nat Cell Biol 4:394–8.

Raiborg C, Bache KG, Mehlum A, et al. (2001a). Hrs recruits clathrin to early endosomes. EMBO J 20:5008–21.

Raiborg C, Bremnes B, Mehlum A, et al. (2001b). FYVE and coiled-coil domains determine the specific localisation of Hrs to early endosomes. J Cell Sci 114:2255–63.

Raiborg C, Malerød L, Pedersen NM, Stenmark H. (2008). Differential functions of Hrs and ESCRT proteins in endocytic membrane trafficking. Exp Cell Res 314:801–13.

Raiborg C, Stenmark H. (2009). The ESCRT machinery in endosomal sorting of ubiquitylated membrane proteins. Nature 458:445–52.

Rauch S, Martin-Serrano J. (2011). Multiple interactions between the ESCRT machinery and arrestin-related proteins: implications for PPXY-dependent budding. J Virol 85:3546–56.

Raymond CK, Howald-Stevenson I, Vater CA, Stevens TH. (1992). Morphological classification of the yeast vacuolar protein sorting mutants: evidence for a prevacuolar compartment in class E vps mutants. Mol Biol Cell 3:1389–402.

Reggiori F, Pelham HR. (2001). Sorting of proteins into multivesicular bodies: ubiquitin-dependent and -independent targeting. EMBO J 20: 5176–86.

Ren J, Kee Y, Huibregtse JM, Piper RC. (2007). Hse1, a component of the yeast Hrs-STAM ubiquitin-sorting complex, associates with ubiquitin peptidases and a ligase to control sorting efficiency into multivesicular bodies. Mol Biol Cell 18:324–35.

Ren X, Hurley JH. (2010). VHS domains of ESCRT-0 cooperate in high-avidity binding to polyubiquitinated cargo. EMBO J 29:1045–54.

Ren X, Hurley JH. (2011). Structural basis for endosomal recruitment of ESCRT-I by ESCRT-0 in yeast. EMBO J 30:2130–9.

Ren X, Kloer DP, Kim YC, et al. (2009). Hybrid structural model of the complete human ESCRT-0 complex. Structure 17:406–16.

Richter C, West M, Odorizzi G. (2007). Dual mechanisms specify Doa4-mediated deubiquitination at multivesicular bodies. EMBO J 26: 2454–64.

Rieder SE, Banta LM, Köhrer K, et al. (1996). Multilamellar endosome-like compartment accumulates in the yeast vps28 vacuolar protein sorting mutant. Mol Biol Cell 7:985–99.

Roll-Mecak A, Vale RD. (2008). Structural basis of microtubule severing by the hereditary spastic paraplegia protein spastin. Nature 451:363–7.

Rossman JS, Jing X, Leser GP, Lamb RA. (2010). Influenza virus M2 protein mediates ESCRT-independent membrane scission. Cell 142:902–13.

Row PE, Liu H, Hayes S, et al. (2007). The MIT domain of UBPY constitutes a CHMP binding and endosomal localization signal required for efficient epidermal growth factor receptor degradation. J Biol Chem 282:30929–37.

Row PE, Prior IA, McCullough J, et al. (2006). The ubiquitin isopeptidase UBPY regulates endosomal ubiquitin dynamics and is essential for receptor down-regulation. J Biol Chem 281:12618–24.

Rue SM, Mattei S, Saksena S, Emr SD. (2008). Novel Ist1-Did2 complex functions at a late step in multivesicular body sorting. Mol Biol Cell 19:475–84.

Russell MR, Shideler T, Nickerson DP, et al. (2012). Class E compartments form in response to ESCRT dysfunction in yeast due to hyperactivity of the Vps21 Rab GTPase. J Cell Sci 125:5208–20.

Rusten TE, Vaccari T, Stenmark H. (2012). Shaping development with ESCRTs. Nat Cell Biol 14:38–45.

Saksena S, Sun J, Chu T, Emr SD. (2007). ESCRTing proteins in the endocytic pathway. Trends Biochem Sci 32:561–73.

Saksena S, Wahlman J, Teis D, et al. (2009). Functional reconstitution of ESCRT-III assembly and disassembly. Cell 136:97–109.

Samson RY, Obita T, Freund SM, et al. (2008). A role for the ESCRT system in cell division in archaea. Science 322:1710–3.

Samson RY, Obita T, Hodgson B, et al. (2011). Molecular and structural basis of ESCRT-III recruitment to membranes during archaeal cell division. Mol Cell 41:186–96.

Sandrin V, Sundquist WI. (2013). ESCRT requirements for EIAV budding. Retrovirology 10:104. doi: 10.1186/1742-4690-10-104.

Sanger JM, Mittal B, Dome JS, Sanger JW. (1989). Analysis of cell division using fluorescently labeled actin and myosin in living PtK2 cells. Cell Motil Cytoskeleton 14:201–19.

Saxton WM, Mcintosh JR. (1987). Interzone microtubule behavior in late anaphase and telophase spindles. J Cell Biol 105:875–86.

Scott A, Chung HY, Gonciarz-Swiatek M, et al. (2005a). Structural and mechanistic studies of VPS4 proteins. EMBO J 24:3658–69.

Scott A, Gaspar J, Stuchell-Brereton MD, et al. (2005b). Structure and ESCRT-III protein interactions of the MIT domain of human VPS4A. Proc Natl Acad Sci U S A 102:13813–18.

Scott PM, Bilodeau PS, Zhdankina O, et al. (2004). GGA proteins bind ubiquitin to facilitate sorting at the trans-Golgi network. Nat Cell Biol 6:252–9.

Seet LF, Liu N, Hanson BJ, Hong W. (2004). Endofin recruits TOM1 to endosomes. J Biol Chem 279:4670–9.

Shenoy SK, Lefkowitz RJ. (2003). Trafficking patterns of beta-arrestin and G protein-coupled receptors determined by the kinetics of beta-arrestin deubiquitination. J Biol Chem 278:14498–506.

Shenoy SK, Xiao K, Venkataramanan V, et al. (2008). Nedd4 mediates agonist-dependent ubiquitination, lysosomal targeting, and degradation of the beta2-adrenergic receptor. J Biol Chem 283:22166–76.

Shiba Y, Katoh Y, Shiba T, et al. (2004). GAT (GGA and Tom1) domain responsible for ubiquitin binding and ubiquitination. J Biol Chem 279:7105–11.

Shields SB, Oestreich AJ, Winistorfer S, et al. (2009). ESCRT ubiquitin-binding domains function cooperatively during MVB cargo sorting. J Cell Biol 185:213–24.

Shields SB, Piper RC. (2011). How ubiquitin functions with ESCRTs. Traffic 12:1306–17.

Shiflett SL, Ward DM, Huynh D, et al. (2004). Characterization of Vta1p, a class E Vps protein in Saccharomyces cerevisiae. J Biol Chem 279:10982–90.

Shih SC, Katzmann DJ, Schnell JD, et al. (2002). Epsins and Vps27p/Hrs contain ubiquitin-binding domains that function in receptor endocytosis. Nat Cell Biol 4:389–93.

Shim JH, Xiao C, Hayden MS, et al. (2006). CHMP5 is essential for late endosome function and down-regulation of receptor signaling during mouse embryogenesis. J Cell Biol 172:1045–56.

Shim S, Kimpler LA, Hanson PI. (2007). Structure/function analysis of four core ESCRT-III proteins reveals common regulatory role for extreme C-terminal domain. Traffic 8:1068–79.

Shim S, Merrill SA, Hanson PI. (2008). Novel interactions of ESCRT-III with LIP5 and VPS4 and their implications for ESCRT-III disassembly. Mol Biol Cell 19:2661–72.

Skalicky JJ, Arii J, Wenzel DM, et al. (2012). Interactions of the human LIP5 regulatory protein with endosomal sorting complexes required for transport. J Biol Chem 287:43910–26.

Slagsvold T, Aasland R, Hirano S, et al. (2005). Eap45 in mammalian ESCRT-II binds ubiquitin via a phosphoinositide-interacting GLUE domain. J Biol Chem 280:19600–6.

Solomons J, Sabin C, Poudevigne E, et al. (2011). Structural basis for ESCRT-III CHMP3 recruitment of AMSH. Structure 19:1149–59.

Spitzer C, Schellmann S, Sabovljevic A, et al. (2006). The *Arabidopsis* elch mutant reveals functions of an ESCRT component in cytokinesis. Development 133:4679–89.

Stahelin RV, Long F, Diraviyam K, et al. (2002). Phosphatidylinositol 3-phosphate induces the membrane penetration of the FYVE domains of Vps27p and Hrs. J Biol Chem 277:26379–88.

Stefani F, Zhang L, Taylor S, et al. (2011). UBAP1 is a component of an endosome-specific ESCRT-I complex that is essential for MVB sorting. Curr Biol 21:1245–50.

Steigemann P, Gerlich DW. (2009). Cytokinetic abscission: cellular dynamics at the midbody. Trends Cell Biol 19:606–16.

Stenmark H, Parton RG, Steele-Mortimer O, et al. (1994). Inhibition of rab5 GTPase activity stimulates membrane fusion in endocytosis. EMBO J 13:1287–96.

Stringer DK, Piper RC. (2011). A single ubiquitin is sufficient for cargo protein entry into MVBs in the absence of ESCRT ubiquitination. J Cell Biol 192:229–42.

Stuchell-Brereton MD, Skalicky JJ, Kieffer C, et al. (2007). ESCRT-III recognition by VPS4 ATPases. Nature 449:740–4.

Sundquist WI, Schubert HL, Kelly BN, et al. (2004). Ubiquitin recognition by the human TSG101 protein. Mol Cell 13:783–9.

Tanaka N, Kaneko K, Asao H, et al. (1999). Possible involvement of a novel STAM-associated molecule ''AMSH'' in intracellular signal transduction mediated by cytokines. J Biol Chem 274:19129–35.

Teis D, Saksena S, Emr SD. (2008). Ordered assembly of the ESCRT-III complex on endosomes is required to sequester cargo during MVB formation. Dev Cell 15:578–89.

Teis D, Saksena S, Judson BL, Emr SD. (2010). ESCRT-II coordinates the assembly of ESCRT-III filaments for cargo sorting and multivesicular body vesicle formation. EMBO J 29:871–83.

Teo H, Gill DJ, Sun J, et al. (2006). ESCRT-I core and ESCRT-II GLUE domain structures reveal role for GLUE in linking to ESCRT-I and membranes. Cell 125:99–111.

Teo H, Perisic O, González B, Williams RL. (2004). ESCRT-Ii, an endosome-associated complex required for protein sorting: crystal structure and interactions with ESCRT-III and membranes. Dev Cell 7:559–69.

Thompson BJ, Mathieu J, Sung HH, et al. (2005). Tumor suppressor properties of the ESCRT-II complex component Vps25 in *Drosophila*. Dev Cell 9:711–20.

Tsang HT, Connell JW, Brown SE, et al. (2006). A systematic analysis of human CHMP protein interactions: additional MIT domain-containing proteins bind to multiple components of the human ESCRT III complex. Genomics 88:333–46.

Urbanowski JL, Piper RC. (2001). Ubiquitin sorts proteins into the intralumenal degradative compartment of the late-endosome/vacuole. Traffic 2:622–30.

Urbé, S., Mills IG, Stenmark H, et al. (2000). Endosomal localization and receptor dynamics determine tyrosine phosphorylation of hepatocyte growth factor-regulated tyrosine kinase substrate. Mol Cell Biol 20:7685–92.

Vaccari T, Bilder D. (2005). The Drosophila tumor suppressor vps25 prevents nonautonomous overproliferation by regulating notch trafficking. Dev Cell 9:687–98.

von Schwedler UK, Stuchell M, Müller B, et al. (2003). The protein network of HIV budding. Cell 114:701–13.

Votteler J, Sundquist WI. (2013). Virus budding and the ESCRT pathway. Cell Host Microbe 14:232–41.

Ward DM, Vaughn MB, Shiflett SL, et al. (2005). The role of LIP5 and CHMP5 in multivesicular body formation and HIV-1 budding in mammalian cells. J Biol Chem 280:10548–55.

Waterman H, Katz M, Rubin C, *et al*. (2002). A mutant EGF-receptor defective in ubiquitylation and endocytosis unveils a role for Grb2 in negative signaling. EMBO J 21:303–13.

Waterman H, Levkowitz G, Alroy I, Yarden Y. (1999). The RING finger of c-Cbl mediates desensitization of the epidermal growth factor receptor. J Biol Chem 274:22151–4.

Wegner CS, Wegener CS, Malerød L, *et al*. (2010). Ultrastructural characterization of giant endosomes induced by GTPase-deficient Rab5. Histochem Cell Biol 133:41–55.

Weissenhorn W, Poudevigne E, Effantin G, Bassereau P. (2013). How to get out: ssRNA enveloped viruses and membrane fission. Curr Opin Virol 3:159–67.

White SR, Evans KJ, Lary J, *et al*. (2007). Recognition of C-terminal amino acids in tubulin by pore loops in Spastin is important for microtubule severing. J Cell Biol 176:995–1005.

Whiteheart SW, Rossnagel K, Buhrow SA, *et al*. (1994). N-ethylmaleimide-sensitive fusion protein: a trimeric ATPase whose hydrolysis of ATP is required for membrane fusion. J Cell Biol 126:945–54.

Williams RL, Urbé S. (2007). The emerging shape of the ESCRT machinery. Nat Rev Mol Cell Biol 8:355–68.

Wollert T, Hurley JH. (2010). Molecular mechanism of multivesicular body biogenesis by ESCRT complexes. Nature 464:864–9.

Wollert T, Wunder C, Lippincott-Schwartz J, Hurley JH. (2009). Membrane scission by the ESCRT-III complex. Nature 458:172–7.

Wu Y, Vendome J, Shapiro L, *et al*. (2011). Transforming binding affinities from three dimensions to two with application to cadherin clustering. Nature 475:510–13.

Xiao J, Xia H, Yoshino-Koh K, *et al*. (2007). Structural characterization of the ATPase reaction cycle of endosomal AAA protein Vps4. J Mol Biol 374:655–70.

Xiao J, Xia H, Zhou J, *et al*. (2008). Structural basis of Vta1 function in the multivesicular body sorting pathway. Dev Cell 14:37–49.

Xie W, Li L, Cohen SN. (1998). Cell cycle-dependent subcellular localization of the TSG101 protein and mitotic and nuclear abnormalities associated with TSG101 deficiency. Proc Natl Acad Sci U S A 95:1595–600.

Yamakami M, Yoshimori T, Yokosawa H. (2003). Tom1, a VHS domain-containing protein, interacts with tollip, ubiquitin, and clathrin. J Biol Chem 278:52865–72.

Yanagida-Ishizaki Y, Takei T, Ishizaki R, *et al*. (2008). Recruitment of Tom1L1/Srcasm to endosomes and the midbody by Tsg101. Cell Struct Funct 33:91–100.

Yang D, Hurley JH. (2010). Structural role of the Vps4-Vta1 interface in ESCRT-III recycling. Structure 18:976–84.

Yang D, Rismanchi N, Renvoisé B, *et al*. (2008). Structural basis for midbody targeting of spastin by the ESCRT-III protein CHMP1B. Nat Struct Mol Biol 15:1278–86.

Yeo SC, Xu L, Ren J, *et al*. (2003). Vps20p and Vta1p interact with Vps4p and function in multivesicular body sorting and endosomal transport in *Saccharomyces cerevisiae*. J Cell Sci 116:3957–70.

Yokouchi M, Kondo T, Houghton A, *et al*. (1999). Ligand-induced ubiquitination of the epidermal growth factor receptor involves the interaction of the c-Cbl RING finger and UbcH7. J Biol Chem 274:31707–12.

Yu Z, Gonciarz MD, Sundquist WI, *et al*. (2008). Cryo-EM structure of dodecameric Vps4p and its 2:1 complex with Vta1p. J Mol Biol 377:364–77.

Zamborlini A, Usami Y, Radoshitzky SR, *et al*. (2006). Release of autoinhibition converts ESCRT-III components into potent inhibitors of HIV-1 budding. Proc Natl Acad Sci U S A 103:19140–5.

Zhang X, Shaw A, Bates PA, *et al*. (2000). Structure of the AAA ATPase p97. Mol Cell 6:1473–84.

Zhao WM, Seki A, Fang G. (2006). Cep55, a microtubule-bundling protein, associates with centralspindlin to control the midbody integrity and cell abscission during cytokinesis. Mol Biol Cell 17:3881–96.